DETERMINATION OF RESIDUAL STRESS STATE IN STEEL WELDMENTS

A THESIS SUBMITTED TO
THE GRADUATE SCHOOL OF NATURAL AND APPLIED SCIENCES
OF
MIDDLE EAST TECHNICAL UNIVERSITY

BY

HASAN İLKER YELBAY

IN PARTIAL FULFILLMENT OF THE REQUIREMENTS
FOR
THE DEGREE OF MASTER OF SCIENCE
IN
METALLURGICAL AND MATERIALS ENGINEERING

JUNE 2009

Approval of the thesis:

DETERMINATION OF RESIDUAL STRESS STATE
IN
STEEL WELDMENTS

submitted by **HASAN İLKER YELBAY** in partial fulfillment of the requirements for the degree of **Master of Science in Metallurgical and Materials Engineering Department, Middle East Technical University** by

Prof. Dr. Canan Özgen _____
Dean, Graduate School of **Natural and Applied Sciences**

Prof. Dr. Tayfur Öztürk _____
Head of Department, **Metallurgical and Materials Engineering**

Prof. Dr. C. Hakan Gür _____
Supervisor, **Metallurgical and Materials Eng. Dept., METU**

Prof. Dr. Bilgehan Ögel _____
Co-Supervisor, **Metallurgical and Materials Eng. Dept., METU**

Examining Committee Members:

Prof. Dr. Tayfur Öztürk
Metallurgical and Materials Engineering Dept., METU _____

Prof. Dr. C. Hakan Gür
Metallurgical and Materials Engineering Dept., METU _____

Prof. Dr. Rıza Gürbüz
Metallurgical and Materials Engineering Dept., METU _____

Prof. Dr. A. Bülent Doyum
Mechanical Engineering Dept., METU _____

Dr. İbrahim Çam
Central Laboratory, METU _____

Date: 17.06.2009

I hereby declare that all information in this document has been obtained and presented in accordance with academic rules and ethical conduct. I also declare that, as required by these rules and conduct, I have fully cited and referenced all material and results that are not original to this work.

Name, Last name : Hasan İlker YELBAY

Signature :

ABSTRACT

DETERMINATION OF RESIDUAL STRESS STATE

IN

STEEL WELDMENTS

YELBAY, Hasan İlker

M.S., Department of Metallurgical and Materials Engineering

Supervisor: Prof. Dr. C. Hakan Gür

Co Supervisor: Prof. Dr. Bilgehan Ögel

June 2009, 76 pages

The purpose of this study is to estimate the residual stress state in steel weldments by using Magnetic Barkhausen Noise (MBN) technique. For obtaining accurate, fast and continuous residual stress measurements a set up for single pass welded plates was designed and used. In order to convert the MBN values to residual stress values a calibration set up was also designed and a procedure for obtaining calibration curves was developed. After welding of low-C steel plates, residual stresses on heat affected zone (HAZ) and parent metal were measured by MBN technique. The results were verified by the hole drilling method. Microstructural investigation and hardness measurements were also conducted.

Keywords: Welding, Residual stress, Non-destructive Evaluation, Magnetic Barkhausen Noise Technique

ÖZ

KAYNAKLI PLAKALARDA KALINTI GERİLİMLERİN ÖLÇÜLMESİ

YELBAY, Hasan İlker

Yüksek Lisans, Metalurji ve Malzeme Mühendisliği Bölümü

Tez Yöneticisi: Prof. Dr. C. Hakan Gür

Yardımcı Tez Yöneticisi: Prof. Dr. Bilgehan Ögel

Haziran 2009, 76 Sayfa

Bu çalışmanın amacı kaynaklı plakalardaki kalıntı gerilimlerin Manyetik Barkhausen Gürültüsü tekniğiyle ölçülmesidir. Ölçüm sonuçlarının daha hassas, hızlı ve sürekli olmasını sağlamak amacıyla tek paso kaynaklı plaklardaki kalıntı gerilimlerin ölçülmesi için bir düzenek tasarlanmış ve kullanılmıştır. Ölçüm sonuçlarını kalıntı gerilim değerlerine çevirmek için kalibrasyon düzeneği hazırlanmış ve kalibrasyon işlemi için bir prosedür geliştirilmiştir. Düşük karbonlu çeliklerin kaynaklanmasından sonra ısıdan etkilenen bölgede (IEB) ve ana metalde Manyetik Barkhausen Gürültüsü metodu kullanılarak ölçümler gerçekleştirilmiş ve bulunan sonuçlar delik açma metodu ile elde edilen sonuçlar ile doğrulanmıştır. Numunelerde, metalografik inceleme ve sertlik ölçümleri de yapılmıştır.

Anahtar kelimeler: Kaynak, Kalıntı gerilim, Tahribatsız Muayene, Manyetik Barkhausen Gürültüsü Yöntemi

To my family

ACKNOWLEDGEMENTS

First of all, I would like to express my deepest gratitude to my supervisor Prof. Dr. C. Hakan Gür for his guidance, understanding and continuous support throughout the study.

I would also like to thank to Dr. İbrahim Çam for helping with the MBN measurements.

I am very thankful to my colleagues from Welding Technology and Non-destructive Testing Research/Application Center for all their help, support, interest and valuable hints.

I would like to express my gratitude for my family: my parents Hüsnü Yelbay and Hamiyet Yelbay for educating me with aspects from both arts and sciences and being next to me whenever I need throughout my life. My sisters Yasemin Yılmaz for sharing her experience of the dissertation writing endeavor with me, Filiz Küçükgüngör and Burcu Öziç for always supporting and believing in me.

I would also like to express my special thanks to Diba Yılmaz for being next to me and support me throughout the study.

TABLE OF CONTENTS

LIST OF TABLES

LIST OF FIGURES

CHAPTER 1

INTRODUCTION

1.1. General

The existence of magnetism is known since the ancient times and it is one of the oldest inventions in the history of science. The magnetic properties of the natural ferric ferrite (Fe_3O_4) stone which is called lodestone (leading stone) or magnetite were described by Greek philosophers in 800 BC. However, before Greek philosophers there were also some Chinese writings back to 4000 B.C. that mention magnetite. The Chinese were the first who understood and benefited from the directive properties of lodestone at 220 B.C. They used a spoon shaped lodestone to identify the south direction, as seen in Figure 1.1 [1].

Figure 1.1: A spoon shaped lodestone [1]

There were also some writings mentioning that the Indians used the magnetite for healing applications at 600 B.C. [2].

As a result of their wide range of usage and mystery, magnetite and magnetism always took a lot of attention in the history of science and humanity. Besides, being a focus of interest throughout the history, magnetism is still a very important discipline of science today and has numerous application fields in industry. Magnetic Barkhausen noise technique is one of the application fields of magnetism that can be used for measuring residual stresses on magnetic materials.

Residual stresses are vital for industrial materials and products and they should be accurately measured or calculated in order to ensure the final product quality. Tensile residual stresses are detrimental for the material because they decrease the fatigue life of the material. On the other hand, compressive residual stresses are beneficial since they prevent crack initiation and propagation [3].

Most of the engineering materials are designed to endure a specific amount of stress. However, residual stresses are added to the real applied stress values which result in a higher stress value on the material. This may cause an unexpected failure.

On the whole, residual stress management has become an important concept for designing and manufacturing industrial components. Each production step is carefully examined in order to reduce the residual stresses with FEM analyses. Different residual stress patterns occur in each production route. Welding is a vital production process for industry and generates residual stresses at a remarkable level.

1.2. Aim of the Study

Welding is the most used joining technique for industrial applications. Construction of big steel structures like pipelines, dams, ships and bridges require welding techniques. However welding introduces residual stress to the material which might be detrimental for the joint. It is important to measure the distribution of these stresses on welds to ensure the quality of the weld. Because it is observed that most of the crack initiation points are

the high tensile stress areas. After knowing these highly stressed points, it is possible to reduce these stresses by applying mechanical and thermal processes.

MBN technique is a challenging method for cost effective and fast nondestructive measurement of residual stresses. By using Magnetic Barkhausen Noise technique it is possible to detect the high stress areas non-destructively on the weld and heat affected zone. After detecting these areas it is also possible to take precautions before cracking occurs.

The aim of this study is to measure the residual stress state in steel weldments nondestructively by the Magnetic Barkhausen Noise Technique.

CHAPTER 2

THEORY

2.1. Theory of Magnetic Barkhausen Noise

Materials can be classified in various ways in terms of magnetic properties they possess. Different classes of magnetic materials are diamagnetic, paramagnetic, ferrimagnetic and ferromagnetic [4]. The scope of this study will be limited to ferromagnetic materials as the Magnetic Barkhausen Noise technique is only applicable to ferromagnetic materials. Iron (as BCC α ferrite), cobalt, nickel and some rare earth metals like gadolinium are some examples of ferromagnetic materials.

Whether a material can be regarded as magnetic or not depends on its two atomic features which are the orbital motion of electrons around the nucleus and the spin motion of electrons about their own axis. The latter is the main cause of ferromagnetic materials to exhibit ferromagnetic properties. In ferromagnetic materials, spins of electrons are aligned parallel to each other as a result of strong interaction between adjacent spins [4].

Except for natural magnets, ferromagnetic materials are found in non-magnetized state in nature. There is no spontaneous magnetization for a block of ferromagnetic substance. As Weiss suggested in 1907, this is because the block consists of many magnetic domains which are spontaneously magnetized and the direction of magnetization changes from one domain to the other so the resulting magnetization is zero. Therefore, ferromagnetic materials can only be magnetized with the application of an external field. If an external D.C. magnetic field is applied to the

ferromagnetic substance, the magnetization of the sample changes as shown in the Figure 2.1.

During the magnetization of the sample, magnetic moments inside the domains aligned themselves with the direction of the applied field. At the same time the walls of the domain move and change their sizes. There are several different regions in magnetization process. These regions are shown at Figure 2.2.

At the lower applied magnetization force (H) values, the motion of the domain wall is reversible. This region is also called the initial permeability range. When the applied field is increased further, the slope of the line becomes steeper. At this point, the process becomes irreversible. When the applied field is removed in this region, some domain walls return to their original positions but most of them do not. As a result of this, there is a remanent magnetization on the sample. At higher applied magnetization force values, the magnetization value becomes constant. This point is called the saturation point. At this point, all of the magnetic domains align themselves in the direction of applied field [4].

If the applied field is reduced or reversed, magnetization decreases but does not follow its original path back. When the applied field is zero, magnetization does not return to zero value. The remaining magnetization is called remanence. Such irreversible process is called hysteresis and it is an important feature for all ferromagnetic materials (Figure 2.2).

The magnetic domain theory was developed by French physicist Pierre-Ernest Weiss who theorized the existence of domains in ferromagnetic materials. Ferromagnetic materials are composed of domains because of energy minimization requirements. The total energy is the summation of five basic energies.

$$E_{tot} = E_{\text{exchange}} + E_{\text{magnetostatic}} + E_{\text{magnetocrystalline}} + E_{\text{magnetoelastic}} + E_{\text{wall}}$$

Variations in these energies have different effects for the equilibrium of the crystalline lattice in the material. The minimization of all energies at the same time is impossible. As a result, a certain magnetic domain configuration occurs for the minimization of total energy [5, 6].

Weiss suggested that 10^{12}-10^{18} atomic magnetic moments were aligned parallel in these domains. However, he could not experimentally prove his suggestions.

Only about a decade later, it was the German physicist Barkhausen who found the first evidence that ferromagnetic materials consisted of domains and that the magnetic moments in the domains change their orientation with the applied field.

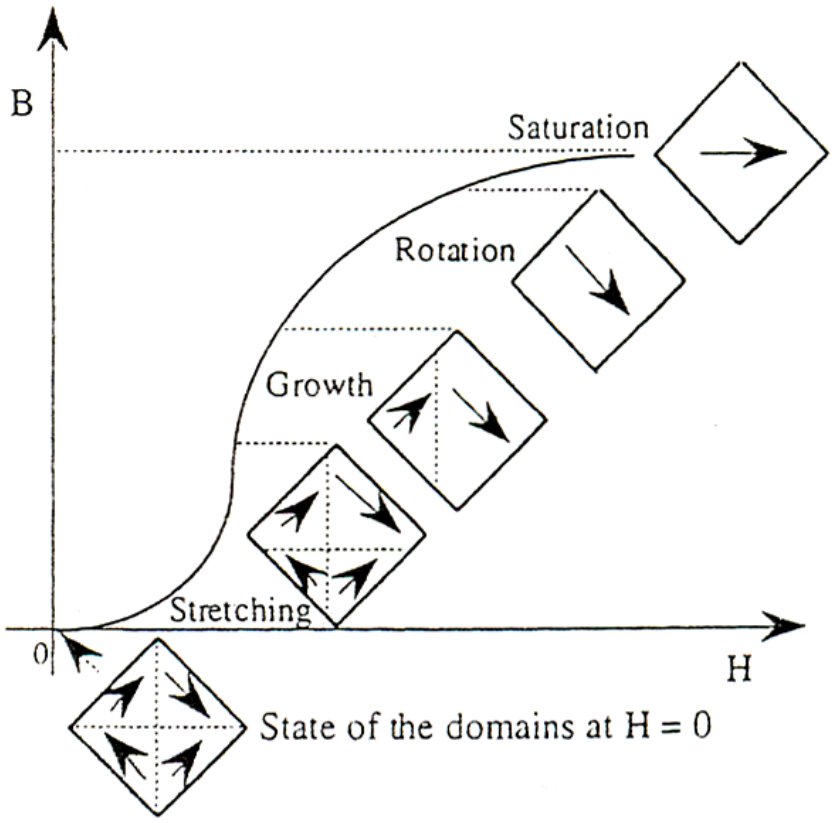

Figure 2.1: Magnetization steps [7]

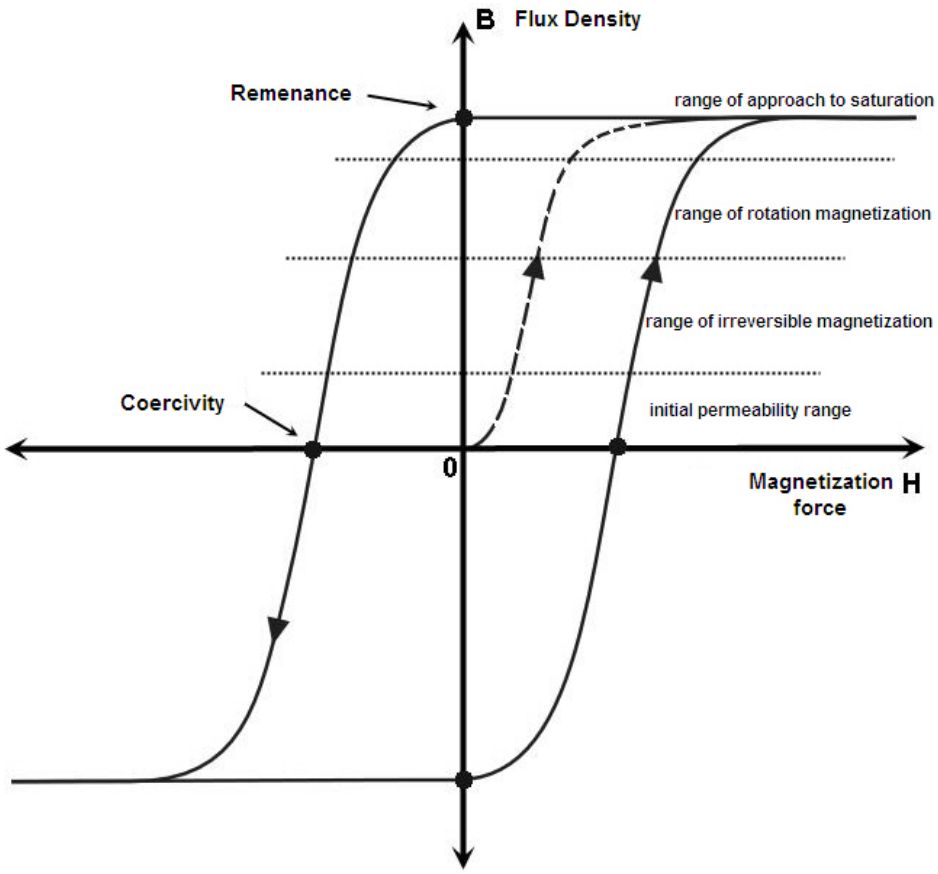

Figure 2.2: Hysteresis curve and regions of magnetization process [4]

> "Iron produces a noise when magnetized. As the magnetomotive force is smoothly varied, the molecular magnets flip in jumps to their new position. Because of this, they generate irregular induction pulses in a coil wound around the sample that can then be heard as a noise in a telephone." [8].

Barkhausen worked mainly on acoustics and magnetism and his studies led to the phenomenon known as the Barkhausen Noise or the Barkhausen Effect. The Barkhausen Effect is described as a series of sudden changes in the size and orientation of ferromagnetic domains. Barkhausen's work provided the experimental proof that was lacking in Weiss's studies [8].

The main aim of Barkhausen was not to prove the Weiss's theory. While he was conducting experiments on acoustics and magnetism he found out that when a magnetic field is applied to a coil of wire wound on a ferromagnetic

material, the sudden change in the magnetization of the material produced current pulses in the coil. These pulses can be amplified to produce a series of sound signals in a loudspeaker. This hissing noise resembles a crackle and is therefore named as the Barkhausen Noise.

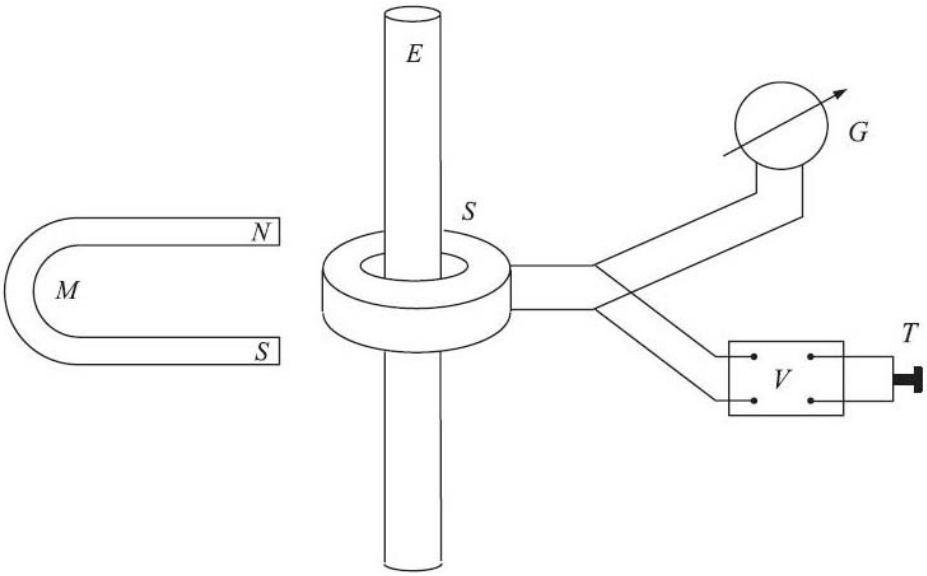

Figure 2.3: Experimental set-up of Barkhausen [8]

Barkhausen found out that the hysteresis curve is not a really linear curve but composed of small jumps as shown in Figure 2.4. Grain boundaries, lattice dislocations, second phase materials (carbides in iron) and impurities in the ferromagnetic material act as an obstacle for the movement of domain walls. By the application of higher magnetization force values, force on the domain wall exceed the restraining force due to pinning sites, so there is an increase in the magnetization in small jumps, which also give rise to hysteresis [4, 7, 8].

There is a transition layer between domains where the direction of the magnetic moment changes as shown in Figure 2.5. These transition layers are named after the Swiss physicist Felix Bloch as Bloch Walls. The thickness of the walls is related to the exchange energy, the

magnetocrystalline (anisotropy) energy and the lattice spacing. The thickness can be calculated by Equation 2.1 where A is the exchange coefficient and K is the anisotropy coefficient [9].

$$\delta := \pi \sqrt{\frac{A}{K}} \tag{2.1}$$

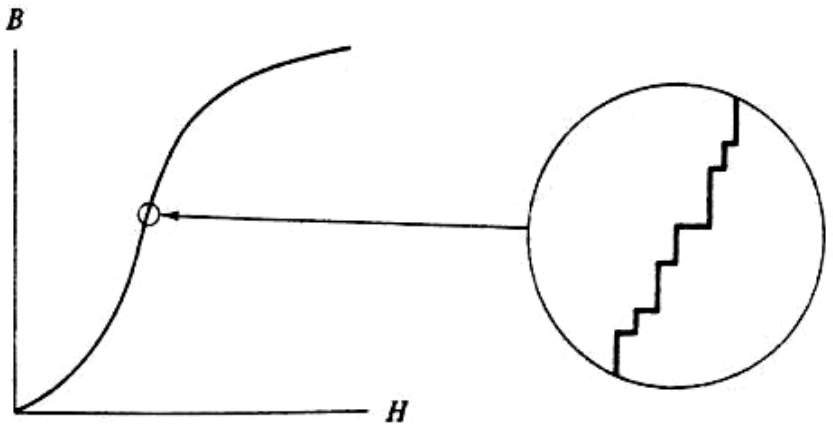

Figure 2.4: Barkhausen jumps along the magnetization [10]

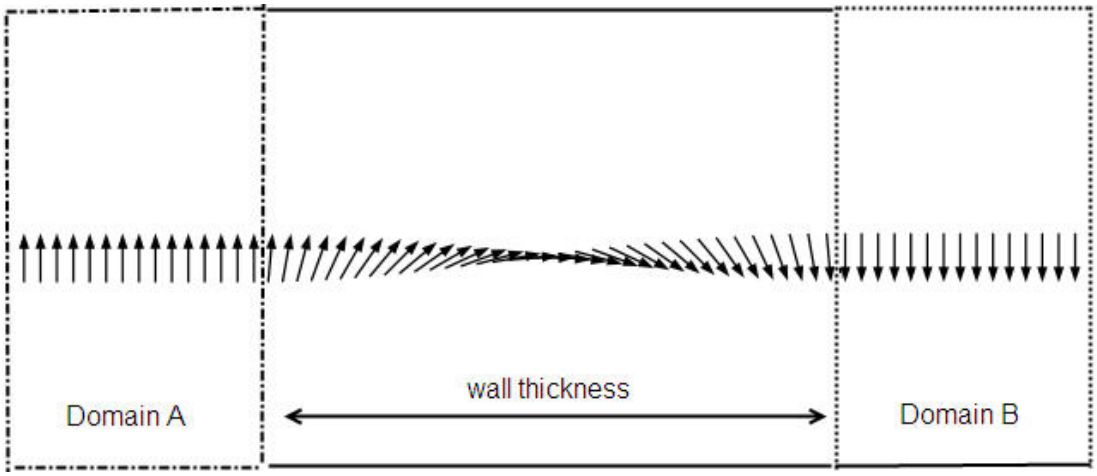

Figure 2.5: Change of the direction of magnetization inside the domain wall

The angular displacements of these walls are generally 90° or 180°. The Magnetic Barkhausen Noise (MBN) signals are generally generated by the motion of the 180° walls because they have a larger average velocity and sweep a larger volume than 90° walls. 90° walls move as well as the 180° walls, however, their contribution to MBN value is small [4, 7, 10].

MBN is sensitive to changes in applied stress, microstructural features and composition of the material. Tensile stresses increase the MBN values whereas compressive stresses decrease these values. With this fact, the measured MBN values can be converted to the real stress values by using calibration curves. This is the main idea of using the Magnetic Barkhausen technique to measure residual stresses in ferromagnetic materials [4, 7, 9, 11].

2.2. Fundamental Information on Residual Stress

Residual stresses are self-equilibrating stresses that remain in the material after the original cause of the stresses (external forces, heat gradient) has been removed. Most of the manufacturing and surface processes produce residual stresses. These processes and the causes of residual stresses are listed at Table 2.1.

Table 2.1: Manufacturing processes and their effects on residual stress [12]

ORIGIN Process	MECHANICAL	THERMAL	METALLURGICAL
Smelting Casting	No	Temperature gradient during cooling	Change of phase
Shot-peening Shock laser treatment Bending Rolling Forging Straightening Extrusion	Heterogeneous plastic deformation between the core and surface of the part	No	No
Grinding Turning Milling Drilling Boring	Plastic deformation due to the removal of chips	Temperature gradient due to heating during machining	Change of phase during machining if the temperature is sufficiently high
Quenching without a phase change	No	Temperature gradient	No
Surface quenching with a phase change (induction, EB, laser, plasma)	No	Temperature gradient	Change of volume due to phase change
Case hardening, nitriding	No	Thermal incompatibility	New chemical component with DV
Welding	Flanging	Temperature gradient	Microstructural change (HAZ)
Brazing	Mechanical incompatibility	Thermal incompatibility	New phase at interphase
Eelctroplating	Mechanical incompatibility	Mechanical incompatibility	Composition of plating depending on bath used
Hot spraying (plasma, laser, Jet Kote)	Mechanical incompatibility, micro-cracking	Thermal incompatibility, temperature gradient	Change of phase during plating
PVD, CVD	Mechanical incompatibility	Mechanical incompatibility	Change of phase
Composite	Mechanical incompatibility	Mechanical incompatibility	No

Main residual stress generating mechanisms are plastic deformations, temperature gradients and metallurgical changes. Generally both of these effects combine to produce residual stresses. Welding and grinding are some examples that contain all of these mechanisms.

In the absence of heat, a plastically deformed plate has a compressive residual stress region at its surface. As shown in Figure 2.6, when a plastic deformation process is applied on the surface, layer A tends to increase its length but layer B restrains it. As a result, compressive residual stress occurs on layer A and these compressive stresses are equilibrated by tensile stresses at layer B. Shot peening process is an example for this condition which is a mechanical process for creating beneficial compressive residual stresses on the materials. There is no effect of thermal gradient and phase transformations on this process.

The other residual stress generating mechanism is the temperature gradient. Due to the effect of temperature gradient, a tensile residual stress region is generated at highly heated areas after cooling. Heated surfaces tend to expand but the material beneath these surface resist this expansion so initially a compressive stress region occurs, but after cooling, A layer tends to shrink but this time B layer resist this shrinkage so finally tensile stress region occurs at layer A (Figure 2.7). Quenching without a phase change can be given as an example for this process.

Also metallurgical changes generate residual stress on the material. This is due to the volume expansion in phase transformations. As a result of martensite phase transformation 2-4% volume expansion occurs. This expansion leads a compressive stress region in transformed area (Figure 2.8).

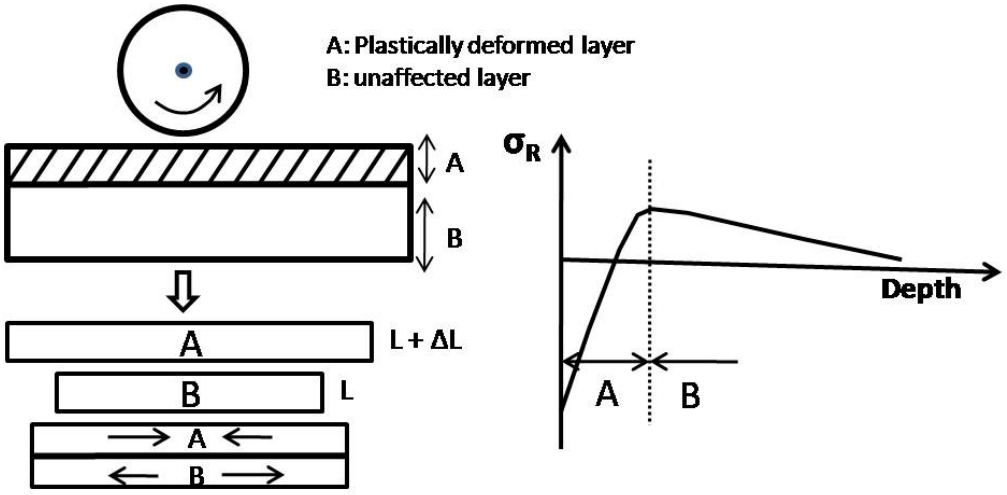

Figure 2.6: Residual stress produced by plastic deformation in the absence of heat [12]

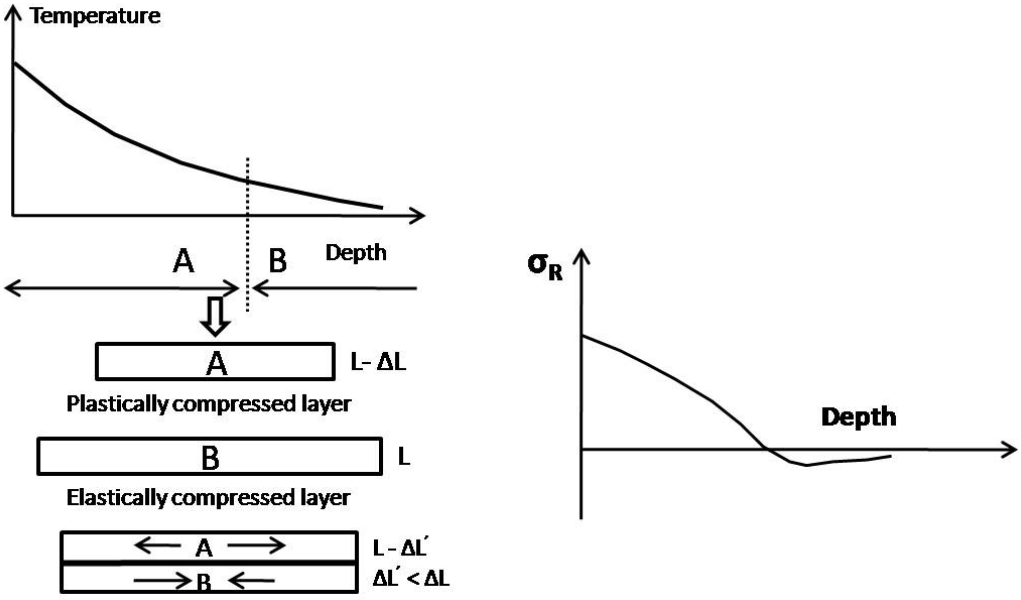

Figure 2.7: Residual stress resulting from exceeding the elastic limit after presence of a temperature gradient [12]

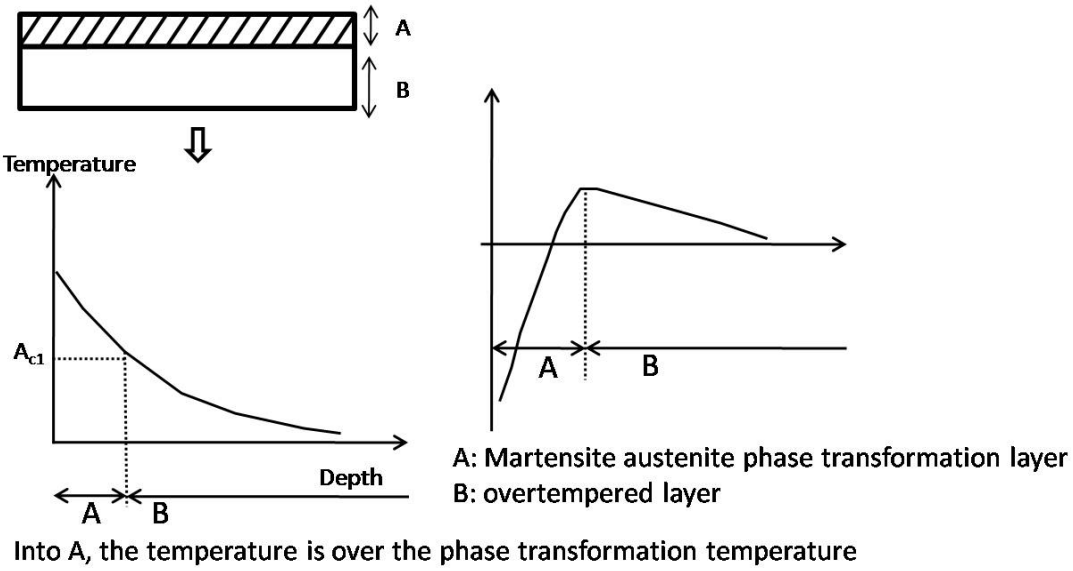

Figure 2.8: Residual stress resulting from change of metallurgical phase [12]

There are three types of residual stresses. Distributions of these stresses over the grains of a specimen are shown in the Figure 2.9. These are macroscopic (type 1) residual stress, microscopic (type 2) residual stress and sub-micro (type 3) residual stress. The macroscopic residual stress is homogeneous and affects a large number of grains in the material. Microscopic residual stress is due to the heterogeneity and anisotropy of each crystal or grain in a polycrystalline material and is nearly homogeneous over a grain or inside a grain. Sub-micro residual stress is equilibrated in several atomic distances in the grain. It is created by all types of crystalline defects like vacancies, dislocations, substitute atoms, stacking faults, interstitial compounds, twin crystals and grain joints [10].

Most mechanical production techniques generally generate macro residual stresses (type 1) as shown in Table 2.2.

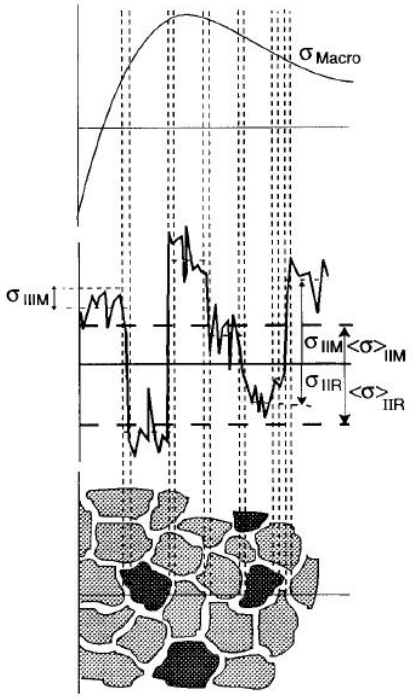

Figure 2.9: Residual stress types [10]

Table 2.2: Sources of macro residual stresses (type 1) [13]

Main sources	Sub sources
Elastic-plastic loading	bending, torsion, tension, compression
Machining	grinding, turning, milling, drilling
Joining	welding, soldering, brazing, adhering
Casting	--
Forming	rolling, drawing, forging, pressing, spinning, shot peening
Heat- treating	quenching, transformation, hardening, case hardening, nitriding
Coating	depositing, cladding, spraying, electroplating, galvanizing

2.3. Residual Stress due to Welding

Welding is defined as "a joining process that produces coalescence of materials by heating them to the welding temperature, with or without the application of pressure or by the application of pressure alone, and with or without the use of filler metal." Welding is a precise, reliable, cost-effective, and “high-tech” method for joining materials. Most of the known objects in modern life, from buildings and bridges, to vehicles, pipe lines, ships, airplanes, computers and medical devices, could not be produced without the use of welding [14].

Welding introduces high heat input to the material being welded. As a result of this, non-uniform heat distribution and phase transformations occur on the material. These changes generate different residual stress patterns for weld region and also in the heat affected zone (HAZ). Shrinkage residual stresses and transformation residual stresses occur on the material as a result of cooling. Each stress generating mechanism has its own effects on the residual stress distribution. In single pass welds relatively simple residual stress distributions are expected, however some variations in the residual stress state can be seen due to inhomogeneous cooling and phase transformations [13].

1.3.1 Shrinkage Residual Stresses

Shrinkage residual stresses are generated during the solidification of the weldment. The longitudinal shrinkage is hindered by the colder and therefore not shrinking areas. If this hindered shrinkage is the only or dominating stress generating process, it results in longitudinal tensile residual stress on the weld which is equilibrated by compressive residual stresses in the heat affected zone and base metal which is away from the weld seam. The magnitude of transverse residual stresses is consistently smaller than the longitudinal stresses [15].

Temperature changes and resulting residual stress distribution during welding is shown schematically along the x-axis of a thin plate at Figure 2.10. The welding arc is moving at a speed v along the x direction.

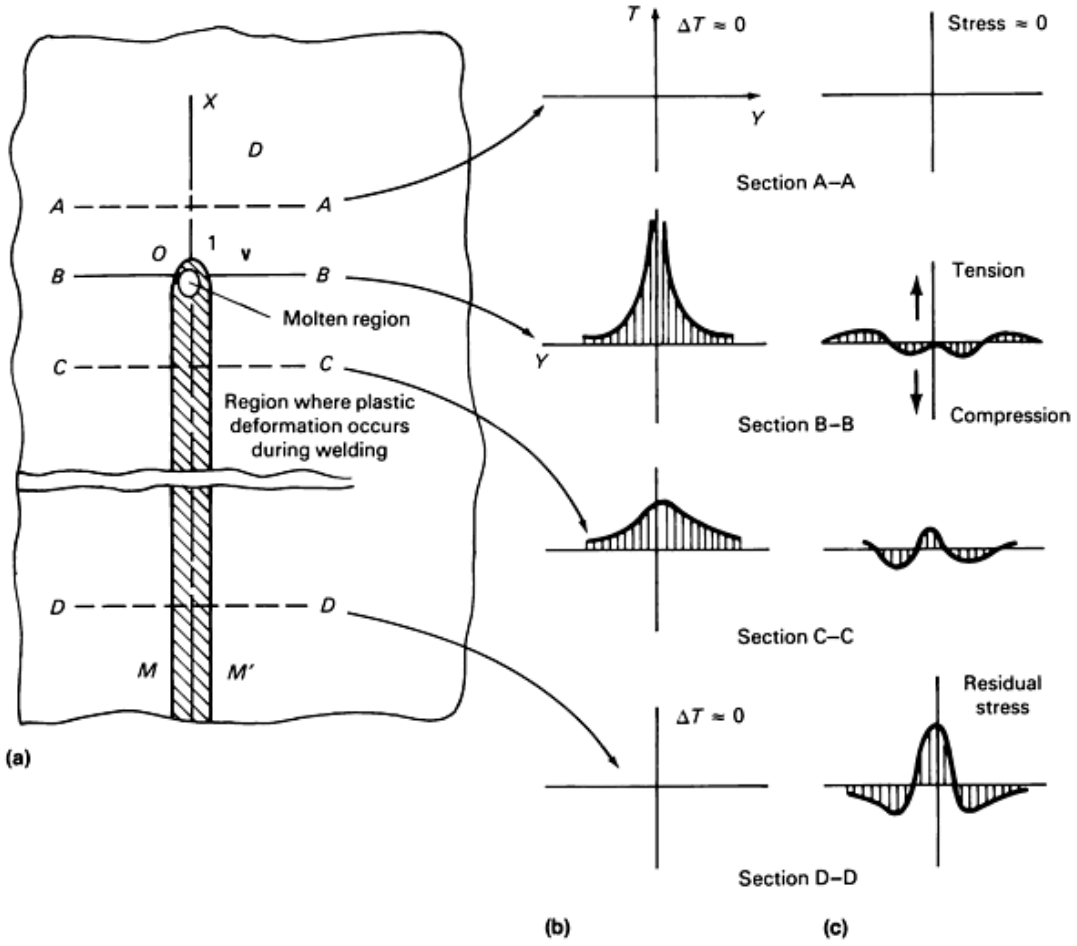

Figure 2.10: Typical temperature and residual stress distributions on a welded plate [16].

At A-A section, the slope of the temperature gradient due to welding is nearly zero (ΔT/ΔY). As a result, there is no residual stress at this section. At B-B section, where the arc is, the slope is very steep and the temperature is very high. This section has a very complicated residual stress pattern. At the molten region, the residual stress value is zero since the molten metal does not support the shear loading. While moving away from the arc, the stresses become compressive because the expansion of the weld metal is compressed by the base metal. These compressive stresses are balanced

with tensile stresses away from the weld centerline. Along the C-C section, the slope becomes less steep. At this point, weld metal and base metal regions are in cooling condition. Because of cooling, shrinkage occurs on the weld metal which leads to tensile stresses. At D-D section, again the slope of the temperature gradient due to welding approaches to zero value. This section has the highest tensile residual stress point after cooling at the weld centerline and these stresses are equilibrated by the compressive stresses at the heat affected zone and base metal [16].

1.3.2 Transformation Residual Stresses

In the regions where the temperature exceeds the eutectoid temperature, the microstructure transforms into austenite. During cooling if austenite transforms to martensite a volume expansion in the transformed area occurs. If the phase transformation is the dominating residual stress generating process, the hindered expansion of the volume results in longitudinal compressive stresses which are equilibrated with tensile residual stresses at a region away from the transforming area [15].

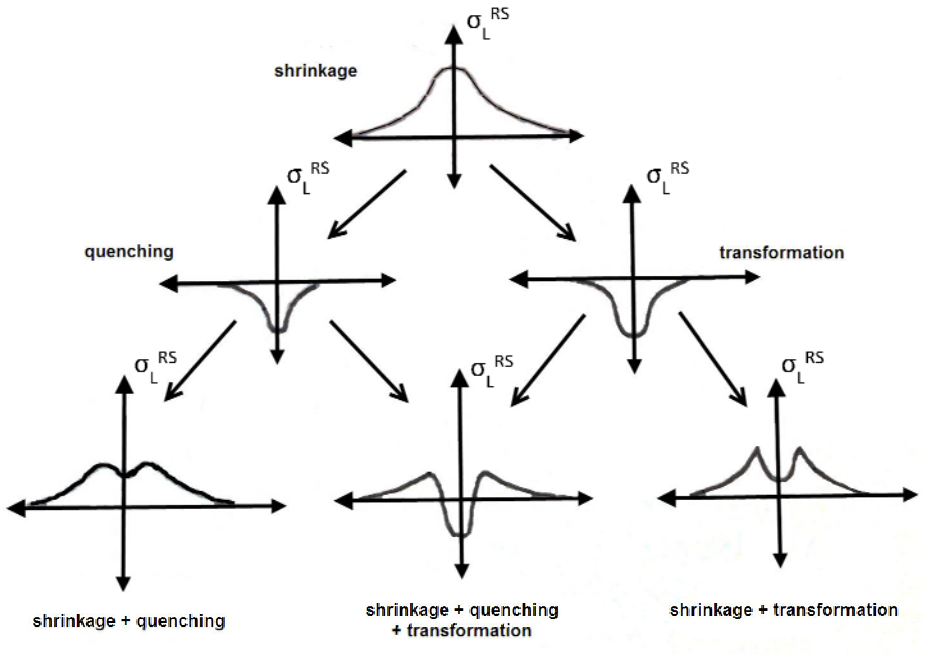

Figure 2.11: Changing of residual stress distribution due to metallurgical processes during welding [13].

With the combination of the residual stresses generating mechanisms different residual stress patterns may be observed on welded materials as shown in Figure 2.11.

1.3.3 Factors Effecting Residual Stress Distribution in Weldments

Welding is a complicated process and contains large amount of parameters. Different process and material parameters have different effects on the residual stress distribution. Process parameters are geometry of the weld, length of a welded part, and heat input on welded region. Material parameters are thickness, type of the material, mechanical properties, microstructure changes and thermal conductivity. The main and most effective parameters are geometry of the weld, length of the weld, heat input, material type and welding parameters.

Geometry of the welded material is important because complex geometries have different cooling rates and as a result complex residual stress distributions are occurred at shown in Figure 2.12.

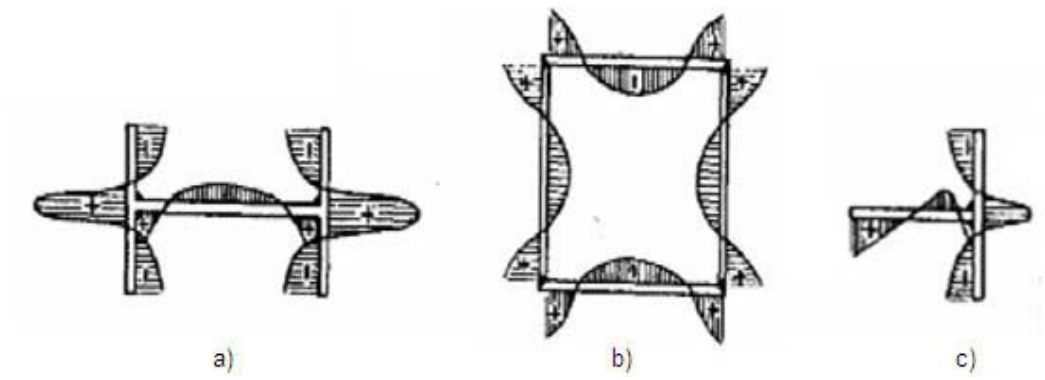

Figure 2.12: Residual stress distributions on a) H-shaped weld, b) box shaped weld, c) T-shaped welds [17].

In the literature it has been reported that longitudinal residual stress becomes a function of the weld length up to 500 mm (Figure 2.13). The welds longer than 500 mm, reach the maximum residual stress values [18].

Heat input in the material increases as the weld length increases. The increase in the heat input causes an increase in residual stress values.

As for the material parameters, different materials show different residual stress distributions because of their different thermal conductivity and microstructure (Figure 2.14).

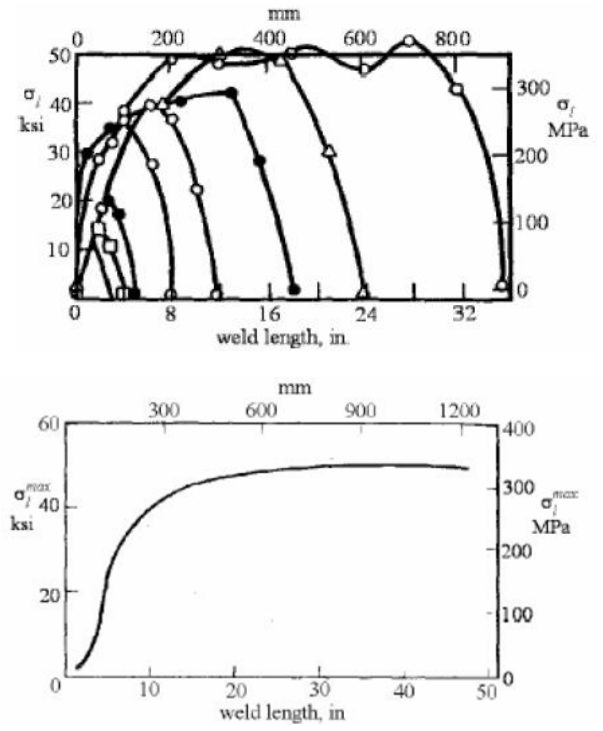

Figure 2.13: Distribution of residual stresses on butt welded plates for different lengths [18]

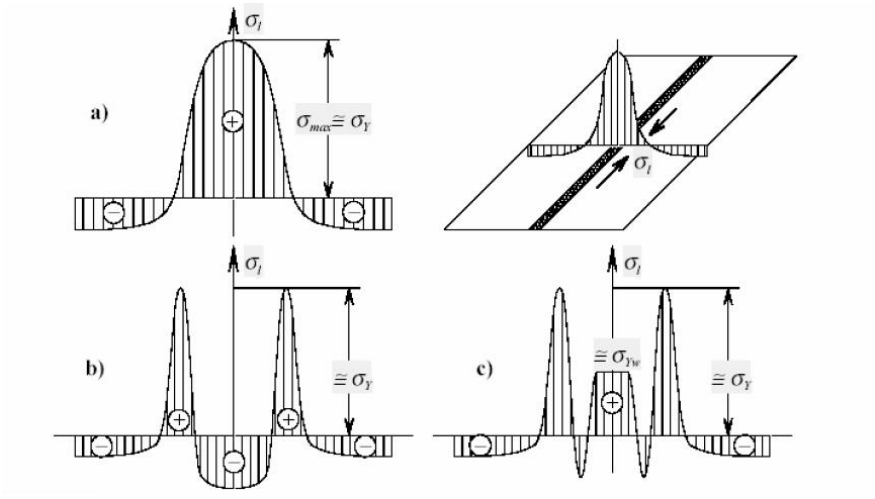

Figure 2.14: Examples of weld-longitudinal stresses; (a) for mild steel, (b) for high-alloy steel with martensitic filler material, (c) for high alloy steel with austenitic filler metal [19].

In the current study, mild steel samples were selected in order to get simple residual stress distributions.

2.4. Residual Stress Measurement Methods

Determination of the residual stress region in welding or other manufacturing techniques is very important for structural integrity assessments. There are several methods for measuring residual stresses. These methods can be classified as destructive methods and non-destructive methods.

1.4.1 Destructive Methods

Destructive methods are mainly based on the strain relieving after a mechanical operation on the sample. These mechanical operations may be drilling a hole, cutting a slit, removing a layer or drilling a circle around a strain gauge. After these mechanical processes, residual stresses reduce with relieving strains in drilled area. These strains can be measured with strain gauges and then converted to stress values by using elasticity theory [10, 20].

Hole drilling method is classified as semi-destructive method since the drilled hole is very small in both diameter and depth. Generally the diameters of the holes are in the range of 1- 4 mm. In this method a smooth hole which is at the center of a strain gauge is carefully drilled with an air pressured drilling machine. By controlling the depth setting, the depth profile of residual stresses can be measured [20, 21]. Hole drilling equipment and strain gauge are shown at Figure 2.15.

ASTM E837 standard defines the procedure for measuring residual stresses with hole drilling method in elastic linear isotropic materials where the stresses do not change significantly with depth. In this condition stresses can be calculated by Equation 2.2. Where, ε_1, ε_2 and ε_3 are the relieved strains after drilling the hole, a and b are geometrically determined and dimensionless parameters which vary with the depth of the hole.

In Equation 2.3, *p* represents the 'volumetric' strain relaxation, where *q* and *t* represent the shear strain components [21].

Equation 2.2 can only be applicable to uniform stress fields. For non-uniform stress fields new analysis procedures were developed. These procedures are integral method and power series method. Integral method gives the best results for non uniform stress fields since it uses the FE calculations and also takes into account of individual contributions to measured strains which identified for each depth increment [21].

$$\sigma_{\min}, \sigma_{\max} = -\left[\left(\frac{p}{\bar{a}(1+\upsilon)}\right) \pm \left(\frac{\sqrt{(q^2+t^2)}}{\bar{b}}\right)\right] E \tag{2.2}$$

$$p = \frac{\varepsilon_3 + \varepsilon_1}{2} \qquad q = \frac{\varepsilon_3 - \varepsilon_1}{2} \qquad t = \frac{\varepsilon_3 + \varepsilon_1 - 2\varepsilon_2}{2} \tag{2.3}$$

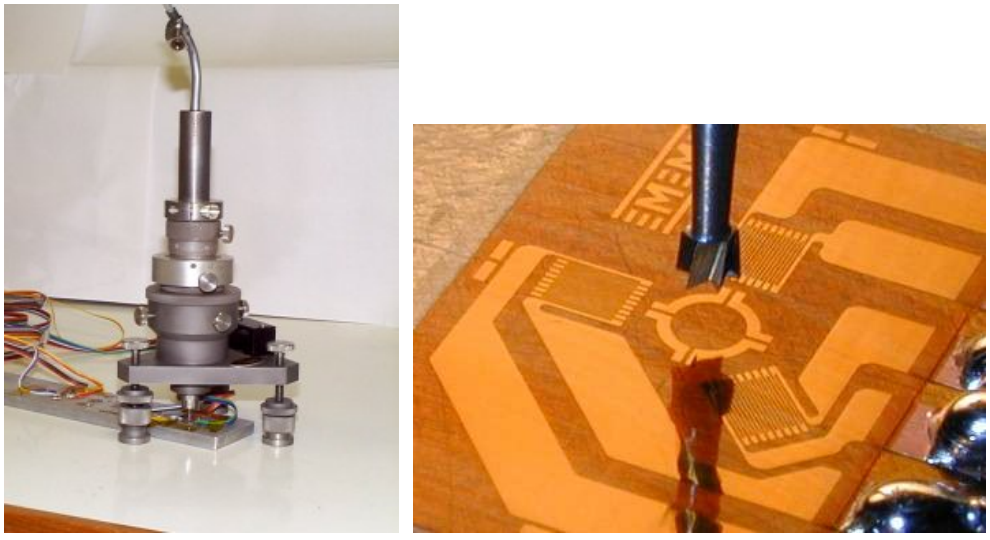

Figure 2.15: Hole drilling equipment and a strain gauge [21]

Destructive tests require basic instruments and theory so they are economic and can easily be applied. However, they are not applicable for in service materials.

1.4.2 Non-destructive Methods

Non-destructive test methods are based on the relationship between physical and crystallographic parameters of a material with the residual stress state. Non destructive test methods are x-ray and neutron diffraction methods, ultrasonic method and magnetic methods.

X-ray and neutron diffraction methods use the spacing between the crystallographic planes as a strain gauge. Both techniques are used for surface residual stress measurements and sensitive to both kind of residual stresses. X-ray method is the most widely used technique and can be combined with layer removal method for measuring depth profile. However this combination becomes destructive. [20, 22]

X-ray diffraction technique gives reliable results however measurement time is relatively long, and devices are expensive.

Ultrasonic method is based on measuring the changes in the ultrasonic wave velocity under the effect of mechanical stresses. These differences can be converted to residual stress values by using calibration curves [23].

Ultrasonic methods require sensitive computerized devices for measuring residual stresses since sound velocity differences due to residual stresses are in the range of nanoseconds.

Magnetic methods rely on the interaction between magnetic properties and elastic strains in ferromagnetic materials. These magnetic properties are; permeability, magnetostriction, hysteresis and Barkhausen Noise. Barkhausen noise signals are sensitive to stress state of the material. Magnetic Barkhausen Noise (MBN) technique is a promising nondestructive method due to its suitability for automation.

CHAPTER 3

LITERATURE REVIEW

A detailed literature survey about residual stress on weldments can be found elsewhere [24, 25]. This part of the thesis has been focused on mainly residual stress measurement on welded components.

K. Masubuchi studied the development of stress and distortion during welding process. He concluded that the metal movement (expansion) during welding is opposite to the distortion, residual stress and distortion takes long time to develop relative to welding time and necessary precautions should be taken in order to reduce the developed residual stresses during welding [26].

J. Gauthier et al. measured the surface residual stresses on a steel specimen by using Magnetic Barkhausen Technique. In their study they used cold-formed steel which is used for construction of transmission lines. The authors compared their results with other destructive and non-destructive testing methods and found ± 25 MPa error with their measurements. They concluded that Magnetic Barkhausen Technique can be used for residual stress measurement [27].

K. Kesevan et al. used the magnetic Barkhausen method for measuring residual stress distribution on a welded mild steel plate. In their study three scanning directions were scanned manually from weld to the base metal. Measured points were 1 mm separated from each other. They found tensile residual stress region near the weld line and compressive residual stress at the heat affected zone. They also compared their results with x-ray diffraction method and found a good correlation [28].

J. Ju et al. investigated the effects of different microstructures on residual stress distribution of a welded API X65 plates. They conducted different calibration curves for different microstructures which occurred in HAZ region. They made their measurements with an interval of 0.5 mm. They compared their results with base metal calibration method in which microstructural changes were ignored. They also compared their result with a destructive residual stress measurement method. A tensile residual stress region was found on the weld centerline. It was also observed that HAZ based calibration method was more accurate than the base metal calibration method [29].

Besides using commercial probes, D.M. Stewart et al. used their own laboratory made probe. AS1548-7-460R steel samples (20 cmx40 cmx7 mm) were joined by a multi-pass arc weld. They measured residual stress distribution with 2 mm. intervals by manual scanning. As a result of their study the maximum MBN values were found at weld region [30].

M. Lindgren used a wheeled MBN sensor for measuring residual stress distribution on welded steel tubes. He compared the MBN results with those of x-ray diffraction method, and found similar results [31].

V. Ochodek made his measurements on API X60 and API X65 welded plates. Measurement points which separated by 30 mm intervals were scanned manually. He found tensile residual stresses at the weld centerlines [32].

V. Ochodek also studied the measurement of residual stresses on API X70 steel plates by magneto elastic method. He found the tensile stresses at the weld centerline which were balanced by the compressive stresses in the heat affected zone. After comparing his results with hole drilling method he observed some deviations [33].

CHAPTER 4

EXPERIMENTAL STUDY

4.1. Material Selection and Industrial Relevance

Measurements of residual stress were carried out on two different steel types. The first one is P355NL2 steel (formerly St52) which is mainly used for construction applications like dam, bridge and ship building. The second steel type is API 5L X70 which is generally used for natural gas and petrol transmission pipelines. For instance, API 5L X70 steel has been used for the construction of the Baku-Tblisi-Ceyhan pipeline (BTC) and pump stations. It was observed that some cracks were occurred at the pump stations in Turkey section. After several examinations like vibration and pressure tests, experts came to the conclusion that the cracks may have been occurred as a result of tensile residual stresses on the welded pipes. High vibrations on the pipes combined with the tensile residual stress and caused these cracks.

Figure 4.1: Cracks on the BTC pump station pumps

The mending of these cracks requires the closure of the whole pipeline however this closure results in both economic and politic problems. Destructive residual stress measurement techniques cannot be used on the in service pipelines. Therefore, the best way to measure residual stresses is to use the non-destructive testing methods such as Magnetic Barkhausen Noise technique.

The compositions and mechanical properties of selected steels are given in the Table 4.1 and Table 4.2 respectively. Both samples were selected in such a way that they should not form martensite phase transformation as a result of thermal activation since the Magnetic Barkhausen Noise decreases in hard materials like martensitic steels.

Table 4.1: Compositions of the steels used

Grade	**P355NL2**	**API 5L X70**
C	0.18	0.064
Si	0.5	0.39
Mn	1.50	1.48
P	0.02	0.013
S	0.01	0.010
N	0.012	-
Ni	-	0.08
Al	0.02	0.031
Cu	0.3	0.16
Ti	0.03	0.020
V	0.1	0.045
Nb	0.05	0.050
Cr	-	0.030

Table 4.2: Mechanical Properties of the steels used

Grade	E (GPa)	σ_y (MPa)
P355NL2	210	355
API 5L X70	213	597

4.2. Preparation of Test Specimens

Two specimens were cut off from P355NL2 steel plates with the dimensions of 300x150x15 mm and 300x150x20 mm. Then, the plates were abrasive machined to get smooth surfaces. Then, U-shaped grooves were machined with a width of 10 mm and depth of 10 mm for 15 mm plate and a width of 10 mm and depth of 8 mm for 20 mm plate at the center of the plates.

For the API 5L X70 plates, two samples were prepared with the dimensions of 300x80x12 mm and 300x80x15 mm. These samples were prepared with the same procedure as mentioned above. After surface preparation, V-shaped grooves opened with a width of 15 mm for 12 mm plate and 10 mm for 15 mm plate. The depth of the grooves was 10 mm.

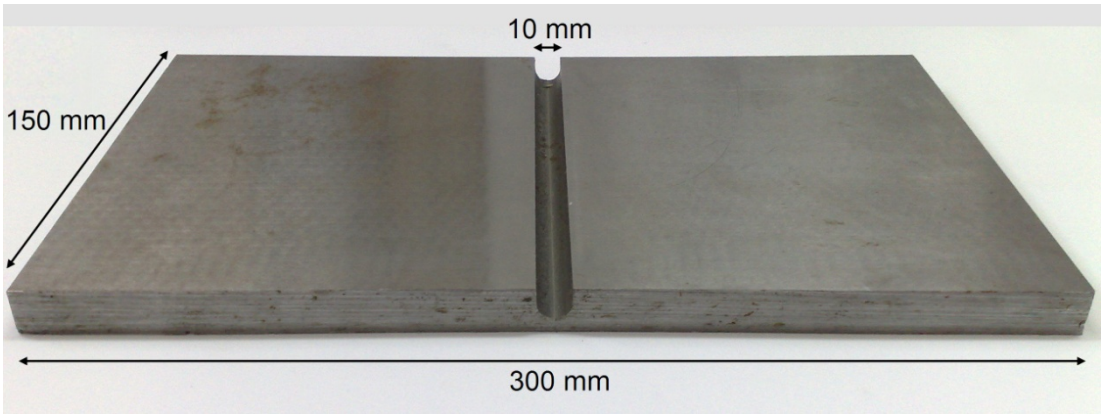

Figure 4.2: U-grooved P355NL2 plates (15 mm)

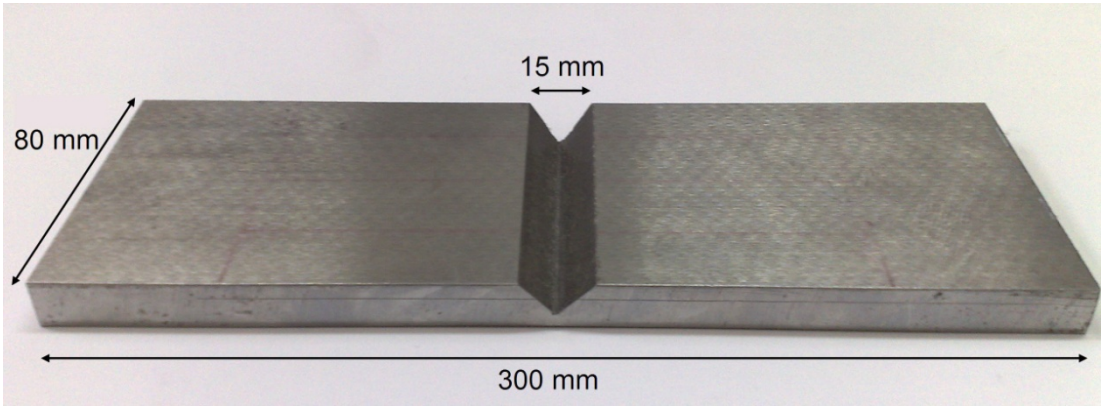

Figure 4.3: V-grooved API 5L X70 plates (12 mm)

4.3. Set-ups for Residual Stress Measurement

Stress measurements were performed using “Rollscan - μscan 500-2” instrument (Figure 4.4) and S1–138–13-01 probe (Figure 4.5). The instrument was used at Rollscan mode. The probe was attached to a motor driven platform for precise and continuous measurement (Figure 4.6). Samples were put on this platform which was driven at a constant speed of 0.2 cm/sec. on the x direction. For each measurement, the position of the probe was carefully aligned in order to get a full contact with the test surface.

Figure 4.4: Magnetic Barkhausen Noise measurement instrument

Figure 4.5: Magnetic Barkhausen noise probe

Figure 4.6: Motor driven instrument for precise and continuous measurement

During MBN measurements a cyclic sinusoidal magnetic field with 125 Hz was used. Received Barkhausen signals were filtered in the range of 70-200 kHz and amplificated by 20 dB for API 5L X70 steel and 10 dB for P355NL2 steel plates. Then the results were analyzed with Rollscan computer software to obtain MBN results.

Before metallographic investigation each specimen was finely grinded, polished and etched with %2 Nital. Hardness measurements were conducted with the standard Vickers hardness measurement system with 10 kg loading. The error of the measurement system was +/- 3 vickers.

Hole drilling measurements were conducted by using RS-200 Milling guide system. This equipment is composed of a hole alignment system and high rpm milling system. CEA-06-062UM-120 strain gauges were used for measuring relieved strains. The measurement system and used strain gages are shown in the Figure 4.7 and 4.8.

Figure 4.7: Hole drilling equipment for residual stress measurement

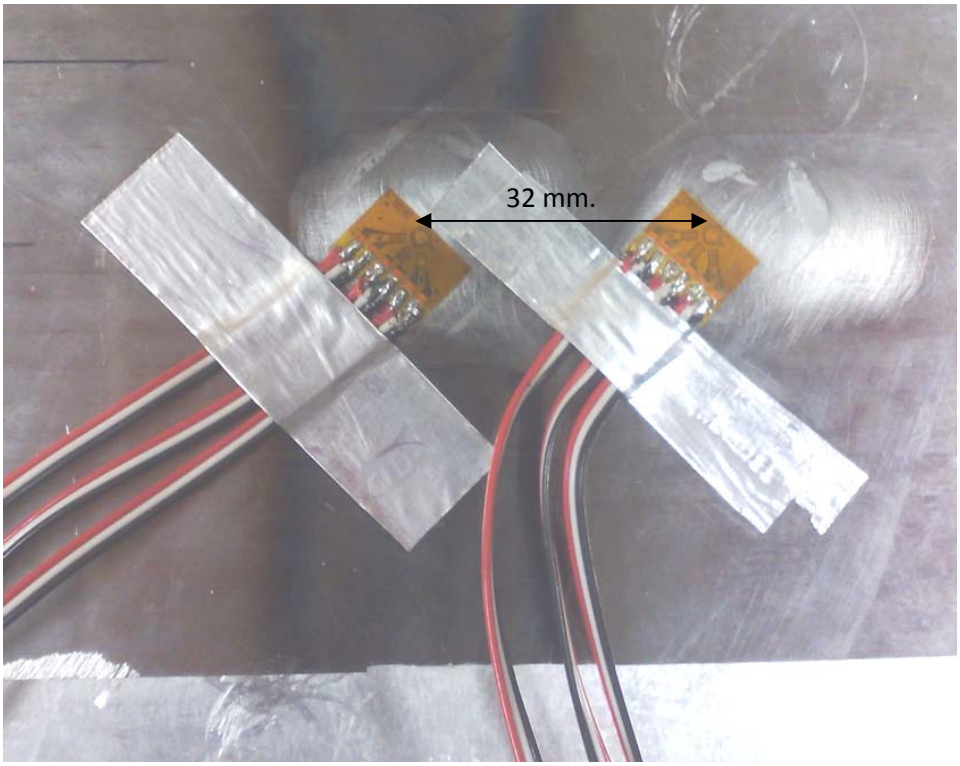

Figure 4.8: Strain gauges and measurement positions

4.4. Test Procedure

Samples were prepared by applying several mechanical processes like grinding and machining. To understand the effects of grinding or machining on residual stress distribution, a trial sample was prepared and MBN values were measured after each step namely grooving, normalizing and welding. The normalizing process was done at 600°C for 2 hours and then the test sample was left for furnace cooling. As shown in Figure 4.9 the effect of grooving on residual stress was nearly negligible since the main contribution of residual stress was the welding process. On the other hand it was observed that normalizing process significantly reduces the MBN value.

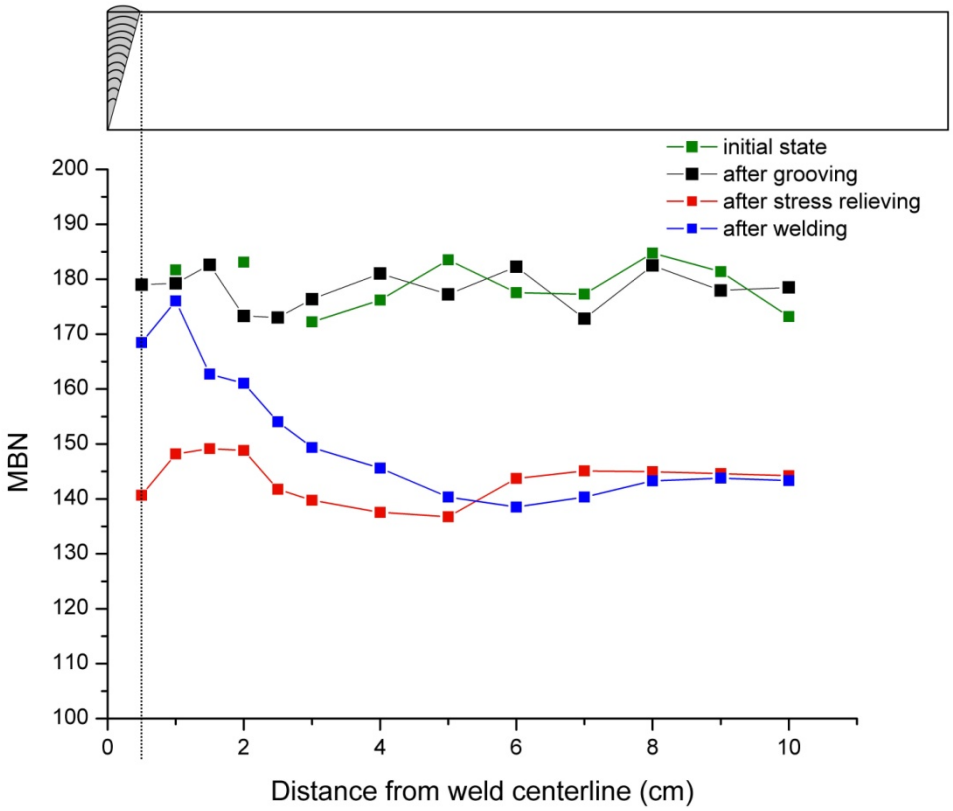

Figure 4.9: Residual stress distributions on the trial test specimen

Before each MBN measurement, demagnetization process was applied to the specimens in order to eliminate the effects of remanent magnetization on the results.

After the base measurements, the welding process was applied with optimum welding parameters as single-pass welding. The welding technique was chosen as the Metal Active Gas (MAG) welding since this technique is widely used for construction applications and also in pipelines. Welding parameters for each welding application is given in Table 4.3. Plates were restrained from their sides to the welding table by tack welding in order to prevent distortion.

Table 4.3: Welding parameters

Material	Voltage	Ampere	Electrode	Welding Method
API 5L X70	22 V	140 A	G3Si1 (SG2)	Metal Active Gas (MAG)
P355NL2	30 V	210 A		

4.5. Calibration Procedure

For the preparation of calibration curves a specific loading set-up was designed to measure the corresponding MBN values for known values of the applied elastic stresses.

Two calibration specimens were prepared for each steel type. In order to eliminate the effects of microstructure on measured MBN values, two calibration procedures were applied. These are base metal based calibration method and HAZ (heat affected zone) based calibration method. For base metal based calibration method calibration specimens were prepared from the base metal and for HAZ based calibration method specimens were cut from the heat affected zone. The dimension of the calibration samples are given in Figure 4.11.

A single element strain gauge was adhered to both of the calibration specimens. Then, the applied strain values were measured by using a strain measurement device (Figure 4.12).

Figure 4.10: Tension/compression loading device

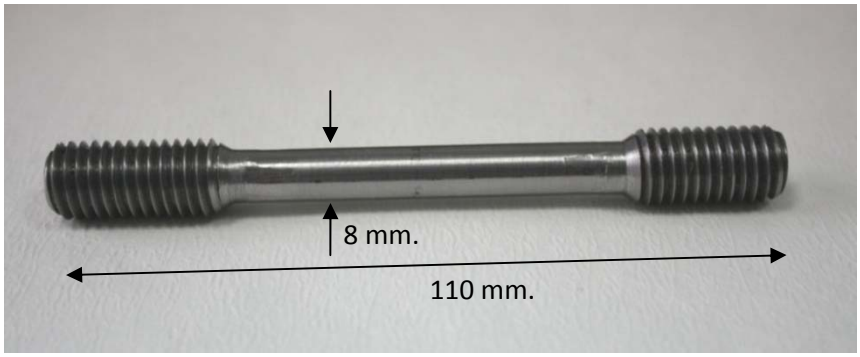

Figure 4.11: Calibration specimen

Figure 4.12: Strain measurement device and calibration specimen

These strain values were converted to the stress values by using elasticity theory. The elastic moduli of the samples were calculated by ultrasonic velocity of longitudinal and transversal waves measurements (Equation 4.1) and checked by tension test results. Elastic moduli of API 5L X70 plate was found as 206 GPa and the elastic moduli of P355NL2 plate was found as 228 GPa.

$$\sigma = \frac{1-2\left(\frac{V_T}{V_L}\right)^2}{2-2\left(\frac{V_T}{V_L}\right)^2} \qquad E = {V_L}^2 \rho \frac{(1+\sigma)(1-2\sigma)}{(1-\sigma)} \qquad (4.1)$$

Where ρ: density, σ: Poisson ratio, E: Elastic modulus, V_T: transverse velocity, V_L: longitudinal velocity [34].

Finally, calibration curves were prepared by using the MBN values and corresponding stress values by using base metal specimens and HAZ specimens. The difference in MBN values of two steels as shown in Figure 4.13 is due to the amplification difference during measurements and microstructural differences of the steels.

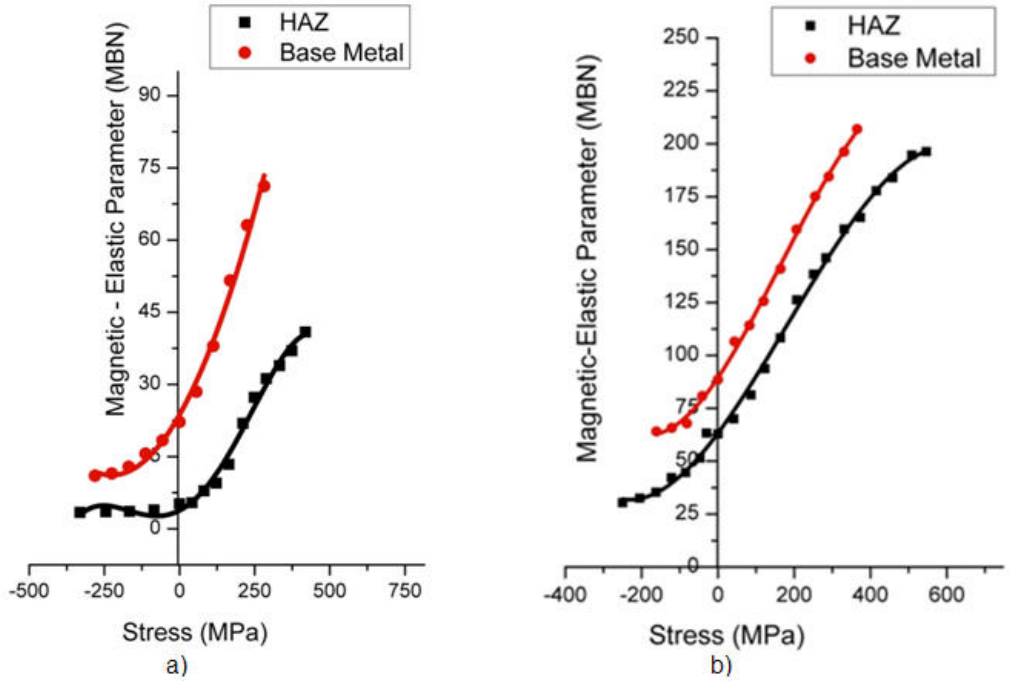

Figure 4.13: Calibration curve for a) P355NL2 steel, b) API 5L X70 steel

CHAPTER 5

RESULTS AND DISCUSSION

5.1. Microstructure Investigation

The micrographs representing the microstructures of the welded plates are given in Figure 5.1 for P355NL2 and Figure 3.2 for API 5L X70 plates. As shown in the figure 5.1, 4 different microstructural regions were observed in P355NL2 plates. Base metal (a) is ferritic-pearlitic structure with a grain size of 10-15 μm. Weld region (b) is composed of acicular ferrite phase with grain size 3-5 μm. HAZ region divided into two parts. In coarse grained part (c) average grain size is 15-20 μm. In fine grained HAZ region (d) grain size is 3-5 μm.

Similar to P355NL2 plate again four different regions are observed in API 5L X70 plates (Figure 5.2). Base metal (a) is ferritic-pearlitic structure and average grain size is 10-15 μm. Weld metal (b) is in acicular ferrite phase with grain size of 5 μm. Coarse grained HAZ region (c) grain size is 25-30 μm and fine grained HAZ region (d) grain size is 3-5 μm.

As mentioned in earlier chapters increasing domain size decreases the MBN values for ferritic microstructures. It was observed that at the coarse grained HAZ regions there was an increase of grain sizes which is responsible for the decrease in MBN values near the weld line.

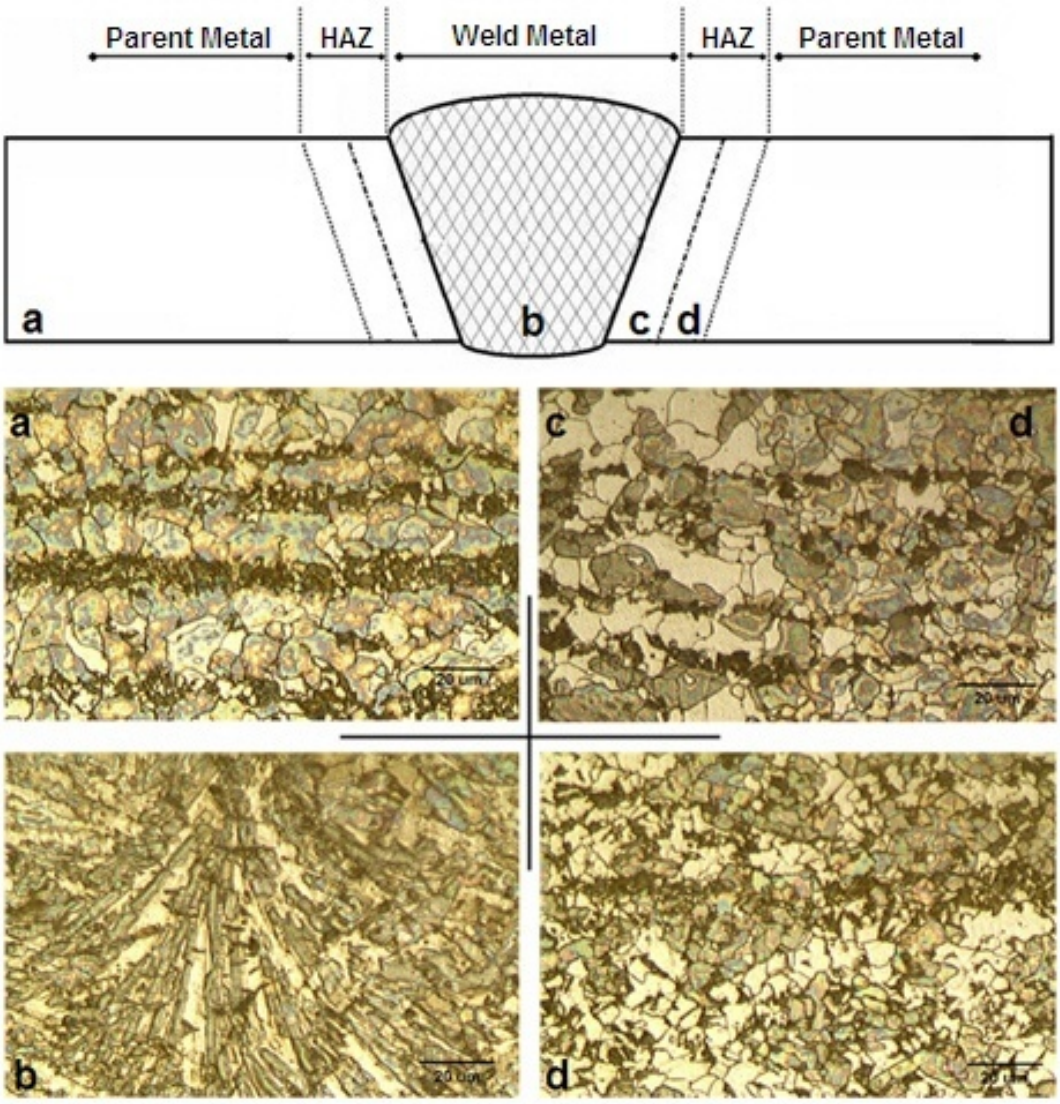

Figure 5.1: Microstructure of P355NL2 steel from parent metal, HAZ and weld metal

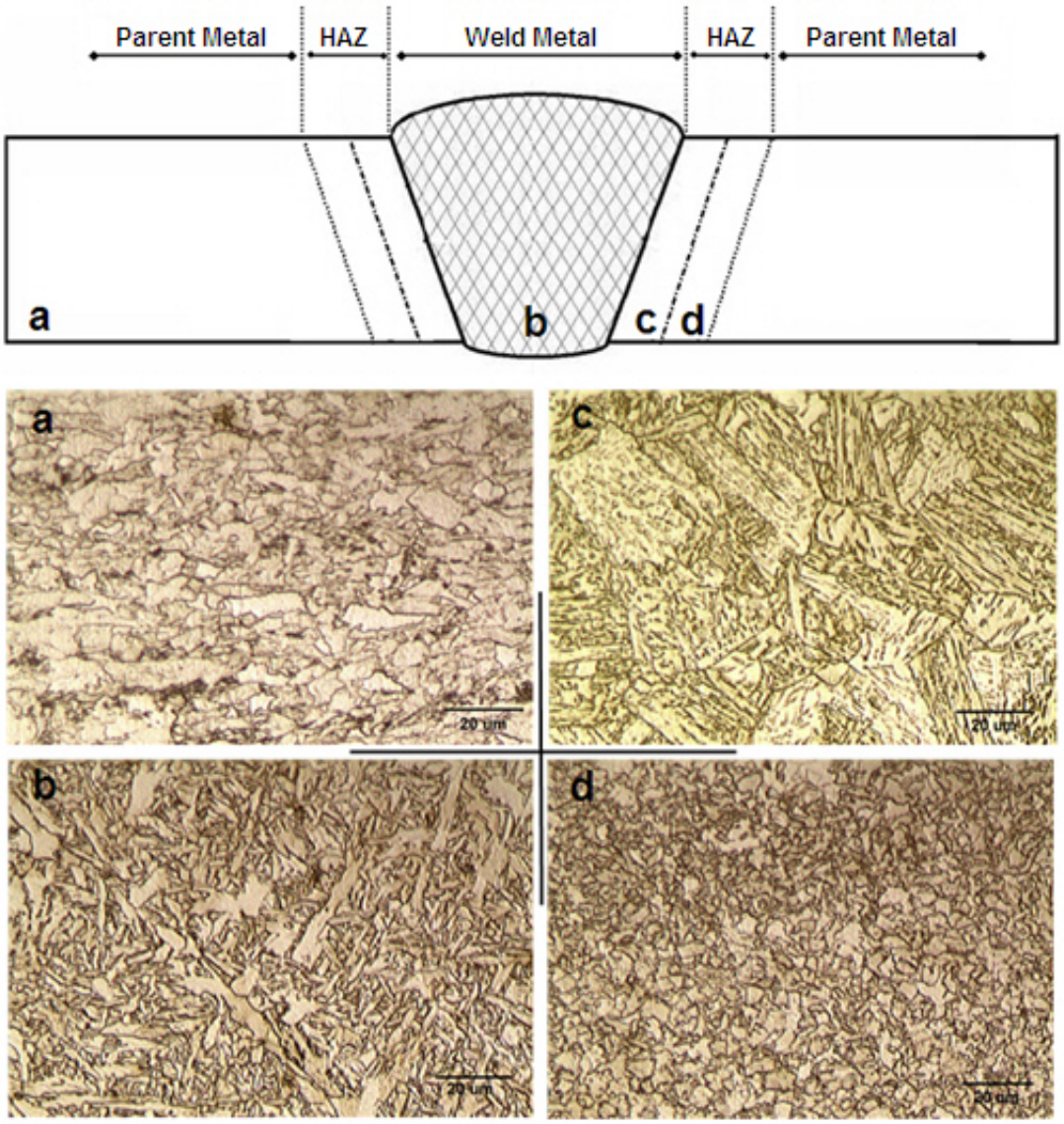

Figure 5.2: Microstructure of API 5L X70 steel from parent metal, HAZ and weld metal

5.2. Hardness Results

Hardness measurements are conducted from front and back surfaces of the plates with 1 mm separation as shown in Figure 5.3. Hardness measurement of API 5L X70 steel from front surface also supports the grain coarsening near the weld line (Figure 5.4). No significant difference was observed from back surface results. As for the P355NL2 plate, the effect of grain coarsening was not observed since the increased carbon content eliminates the decline of hardness values caused by grain coarsening. No significant differences were obtained from back surface results (Figure 5.5).

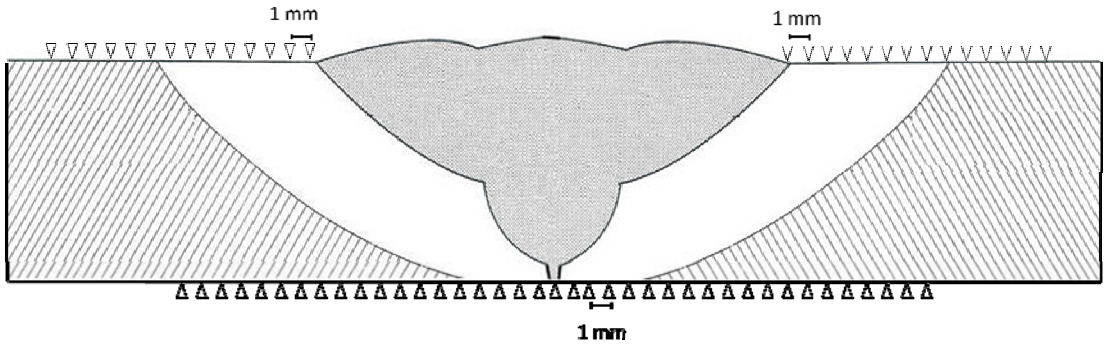

Figure 5.3: Hardness measurement points

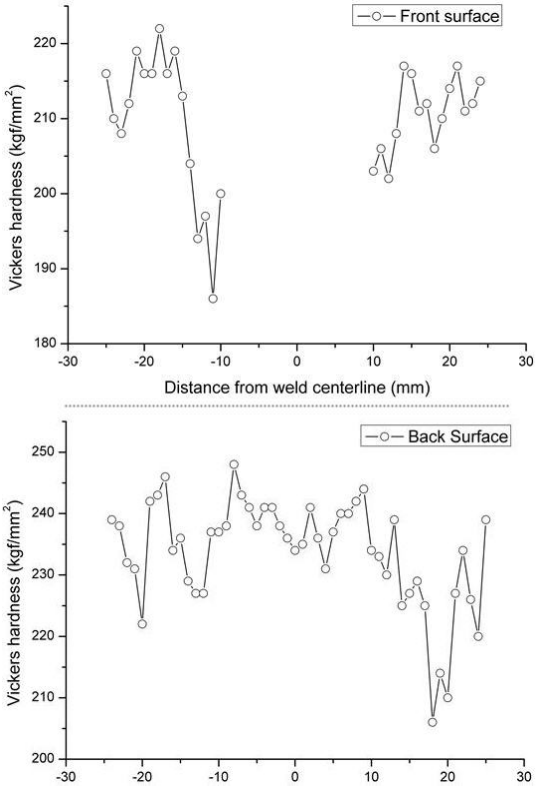

Figure 5.4: Hardness results of API 5L X70 plate

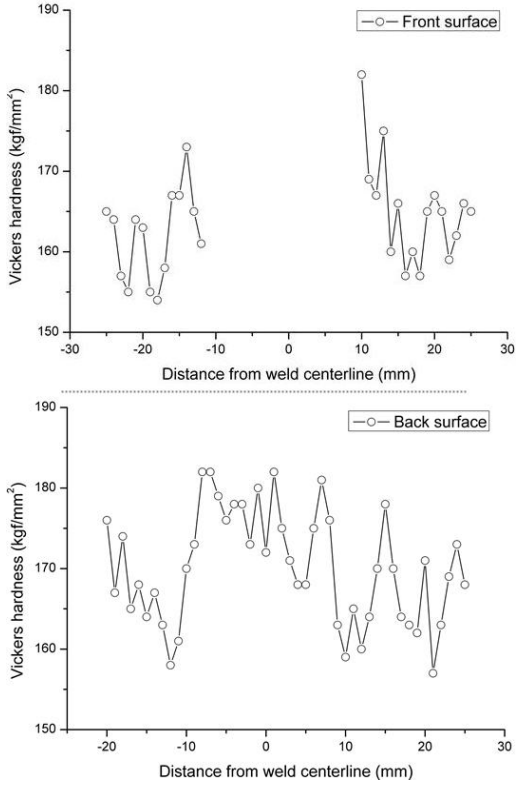

Figure 5.5: Hardness results of P355NL2 plate

5.3. Barkhausen Emission Profiles

MBN measurements were conducted on both sides of the welded plates. Measurement lines are parallel and separated 20 mm from each other (Figure 5.6). For predicting the residual stress distribution behavior of welded plates, raw MBN value results are represented on the schematic drawings. Figures 5.7 and 5.8 show the results of 12 mm API 5L X70 plate from front surface and back surface measurements for three measurement lines. Figures 5.9 and 5.10 represent the MBN profile of 15 mm API 5L X70 plate which has 10 mm width V groove from front and back surfaces for three measurement lines. In Figures 5.11 and 5.12 MBN profiles of 15 mm P355NL2 plate which has 10 mm width U groove were drawn from front and back surfaces for six and seven measurement lines, respectively. Figures 5.13 and 5.14 represent the results of 20 mm P355NL2 steel again from front and back surfaces for six and seven measurement lines, respectively. Raw MBN data distributions of the plates reveal the consistency of the measured data points since for each measurement line more than 1500 data points were obtained.

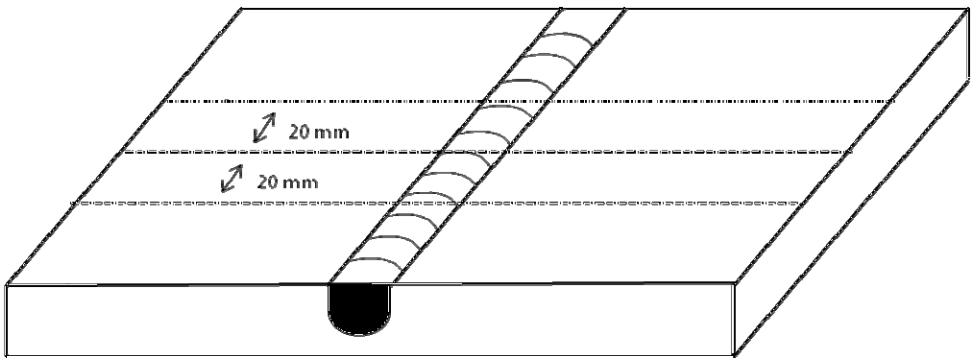

Figure 5.6: Measurement lines for API 5L X70 and P355NL2 steel perpendicular to the weld centerline

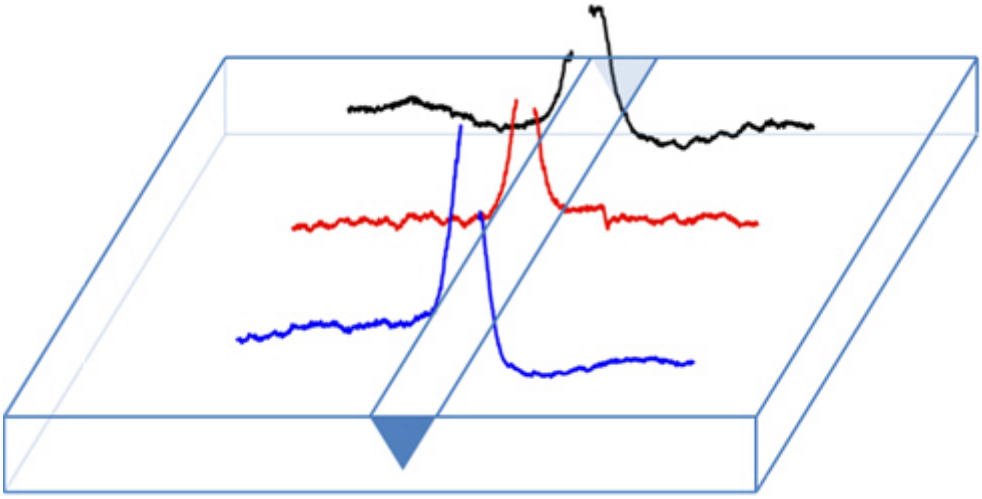

Figure 5.7: MBN profile of 12 mm API 5L X70 plate from front surface

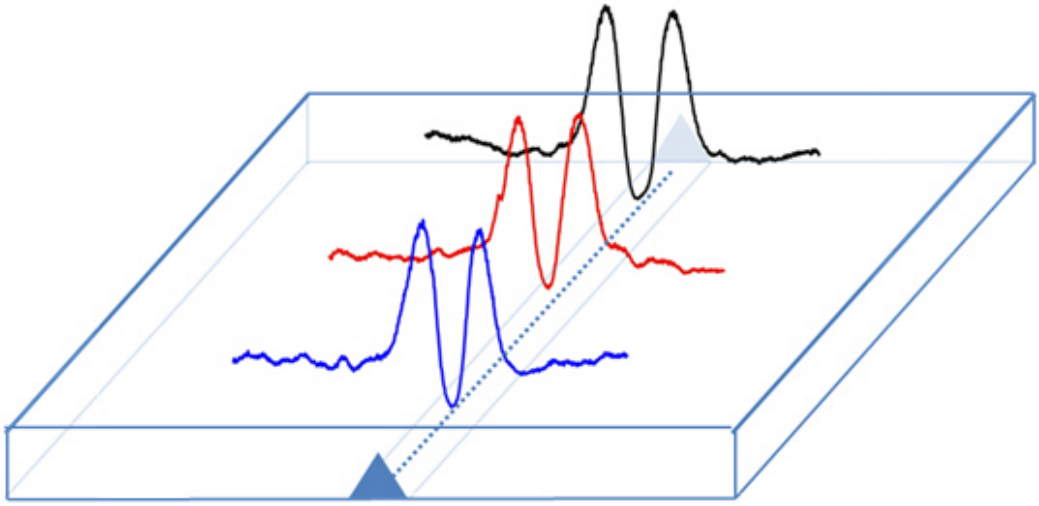

Figure 5.8: MBN profile of 12 mm API 5L X70 plate from back surface

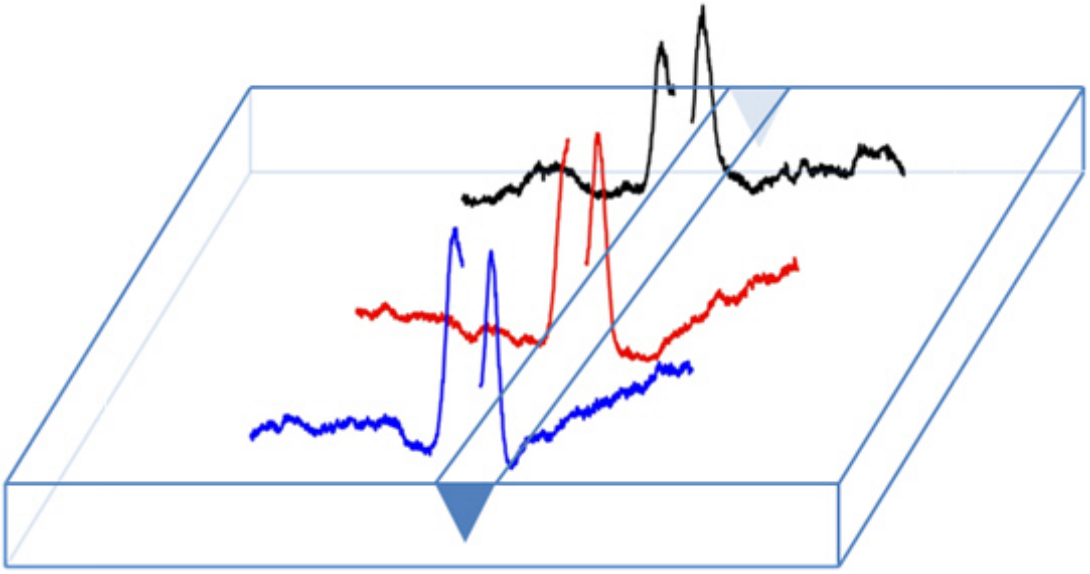

Figure 5.9: MBN profile of 15 mm API 5L X70 from front surface

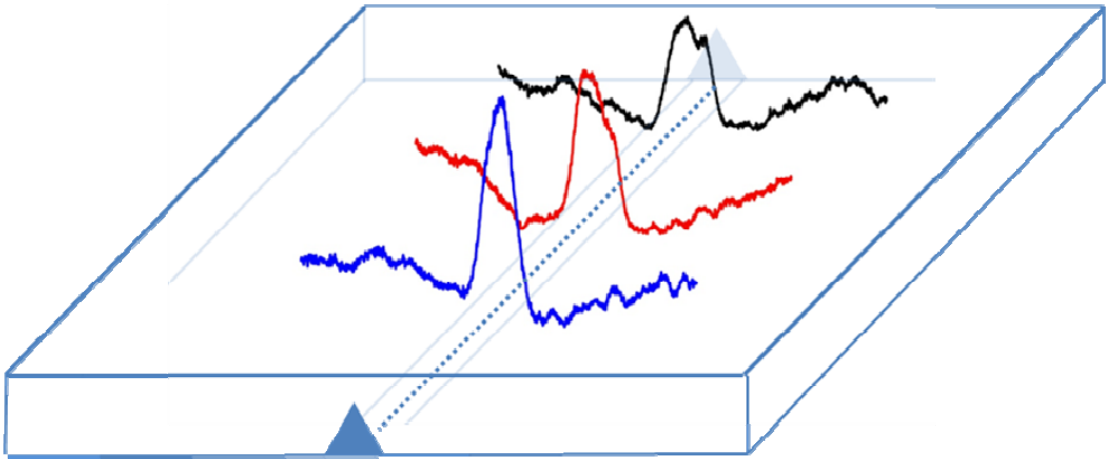

Figure 5.10: MBN profile of 15 mm API 5L X70 from back surface

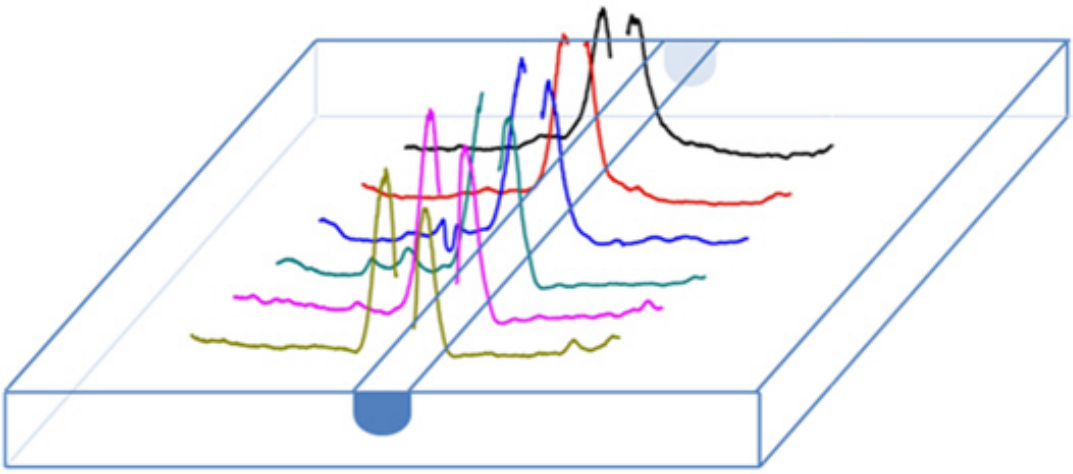

Figure 5.11: MBN profile of 15 mm P355NL2 plate from front surface

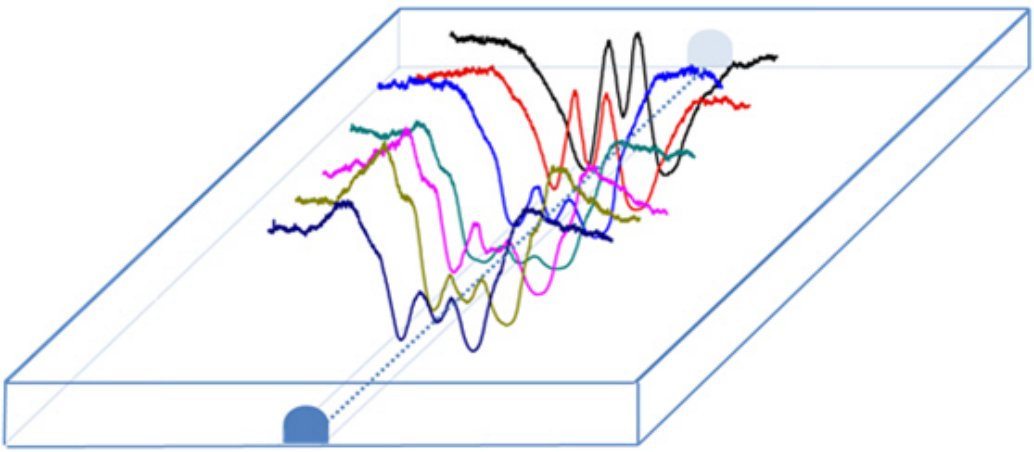

Figure 5.12: MBN profile of 15 mm P355NL2 plate from back surface

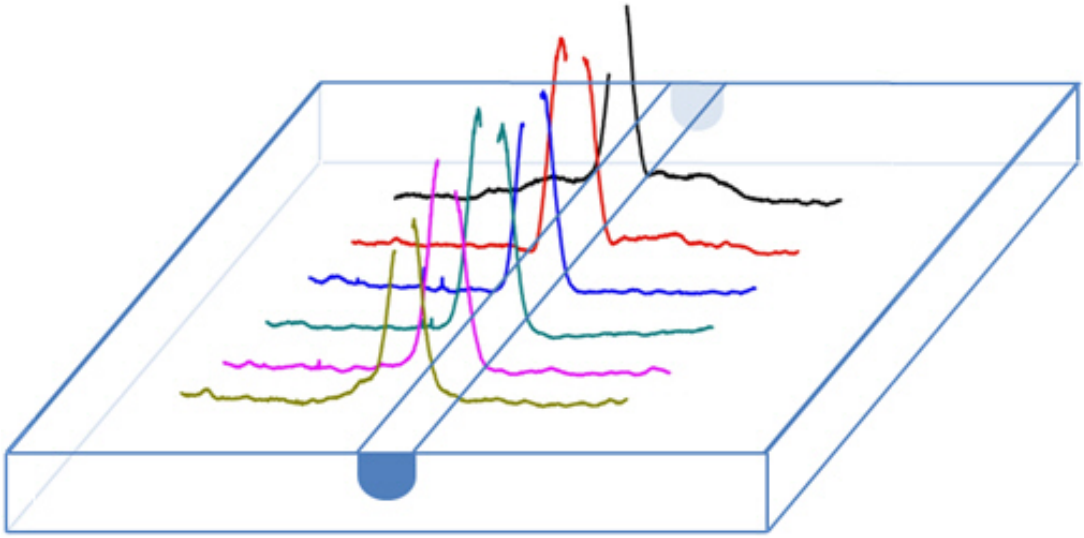

Figure 5.13: MBN profile of 20 mm P355NL2 plate from front surface

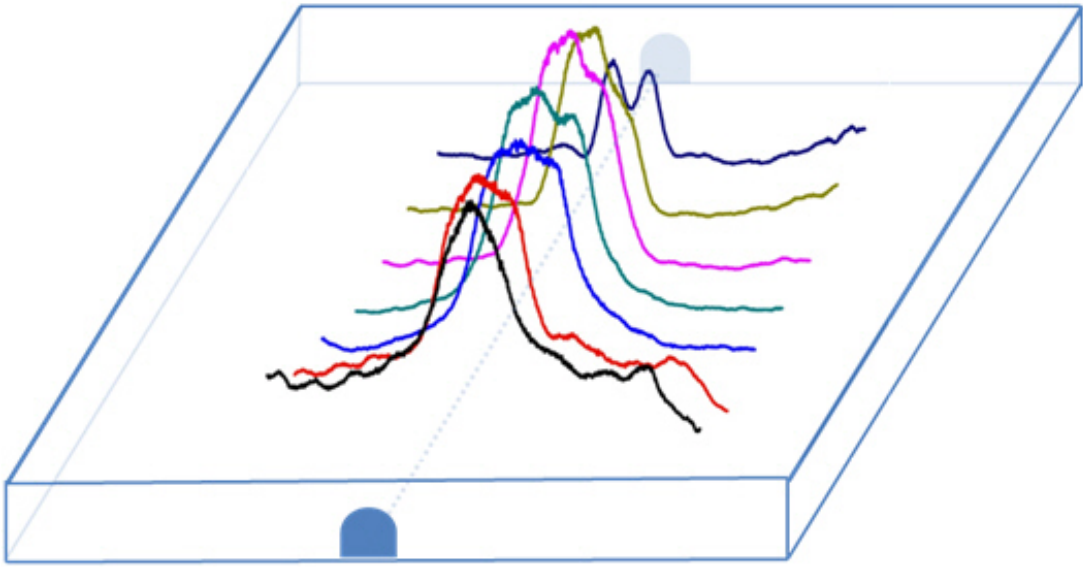

Figure 5.14: MBN profile of 20 mm P355NL2 plate from back surface

5.4. MBN Results for Base Metal Calibration

Two different calibration procedures were used. The first procedure was the base metal calibration technique in which only the base metal calibration curve was used in order to obtain corresponding residual stress result. Figure 5.15 shows longitudinal residual stress results of 15 mm P355NL2 steel from front and back surface at measurement lines 1, 2, 5 and 6. As seen in the Figure 5.15 the plate initially has a compressive stress at front surface. After welding it is seen that a tensile stress region was occurred at HAZ region. The decline of residual stress values near the weld metal is due to the grain coarsening. The back surface of the plate initially has a tensile stress region. However, after welding compressive stress regions occurred. The decline of residual stress values on the center line of the weld is due to combination effects of shrinkage, transformation, and quenching.

The same residual stress distribution was observed for 20 mm P355NL2 plate as shown in Figure 5.16. The main difference between 15 mm and 20 mm P355NL2 plates was observed from back surface results. The decline of the residual stresses occurred on 15 mm steel was not observed in the 3rd, 4th, and 5th measurement lines for 20 mm P355NL2 steel. However, the same effect was observed in 7th measurement line. This decline on the center line of the weld is due to the effect of increasing heat input on the weldment.

The 12 mm API 5L X70 plate initially has a compressive stress region on its surface (Figure 5.17). After welding a tensile stress region occurred similar to 15 and 20 mm P355NL2 steel at the HAZ region. It is impossible to obtain residual stress results from back surface of 12 mm API 5L X70 steel because of high deviation of the residual stress values.

As for 15 mm API 5L X70 plate an increase in residual stress values was observed at HAZ regions (Figure 5.18). The decline of residual stress values that occurred near the weld line region was due to the grain coarsening. From back surface results it is observed that there was an increase at the weld centerline.

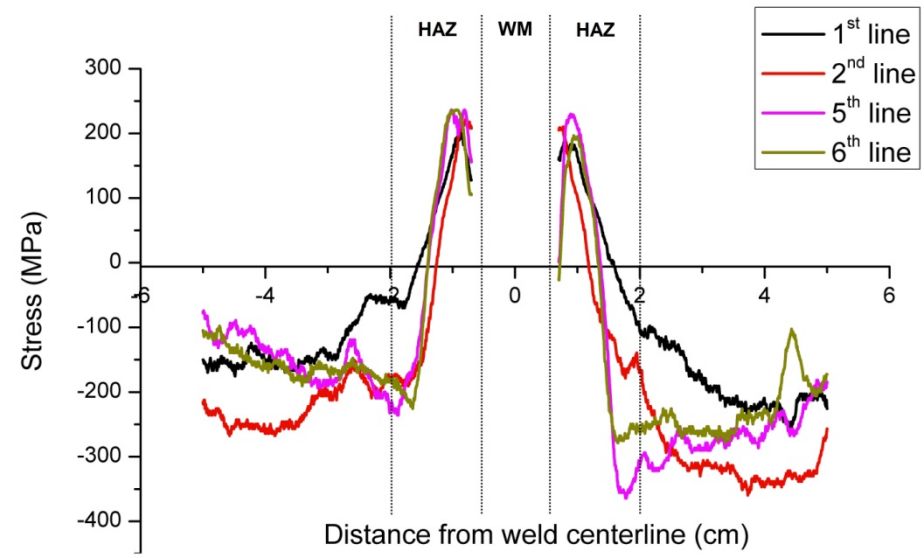

a)

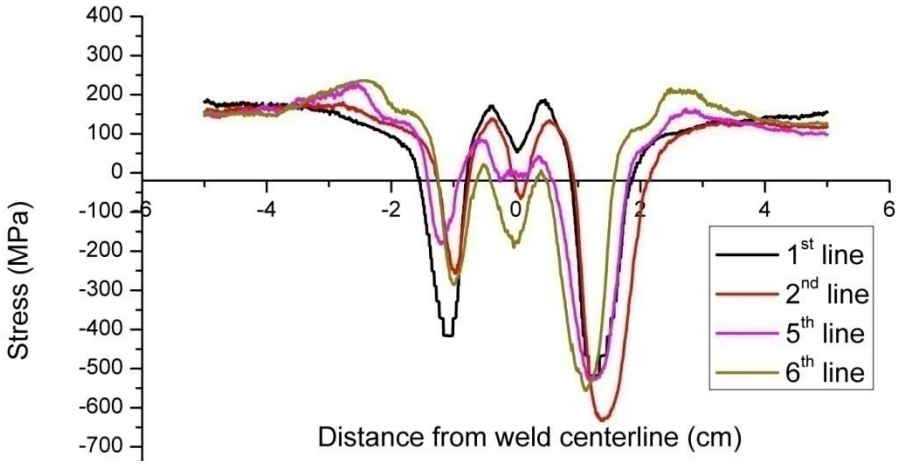

b)

Figure 5.15: Longitudinal residual stress distribution of P355NL2 (15 mm) steel from surface a) and back surface b) at measurement lines 1, 2, 5 and 6.

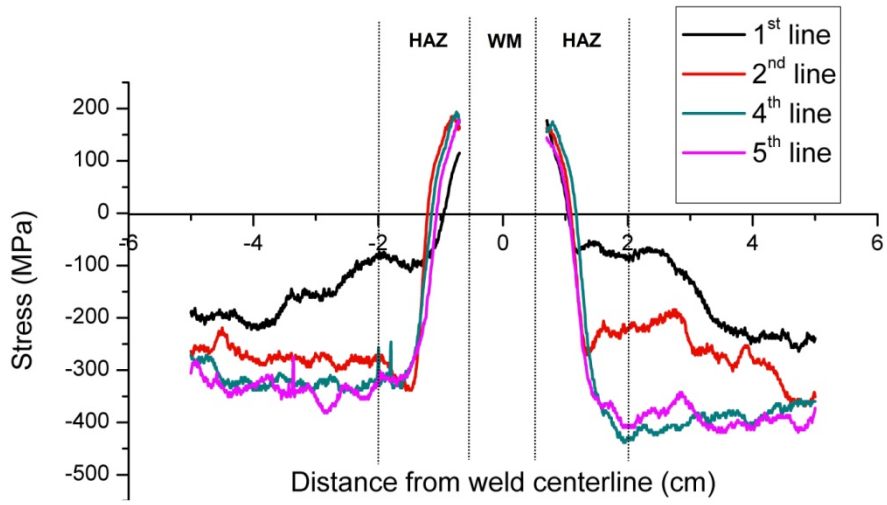

a)

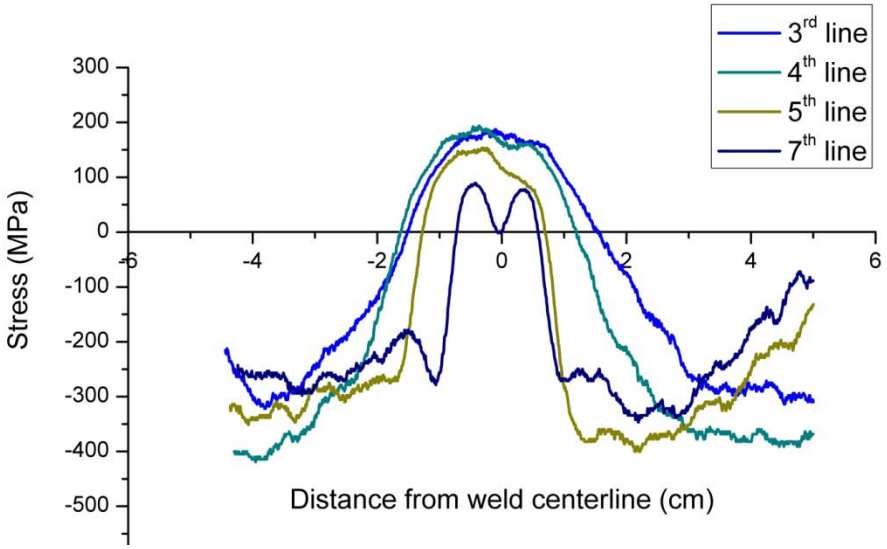

b)

Figure 5.16: Longitudinal residual stress distribution of P355NL2 (20 mm) steel from a) surface at measurement lines 1, 2, 4, 5, and b) back surface at measurement lines 3, 4, 5 and 7.

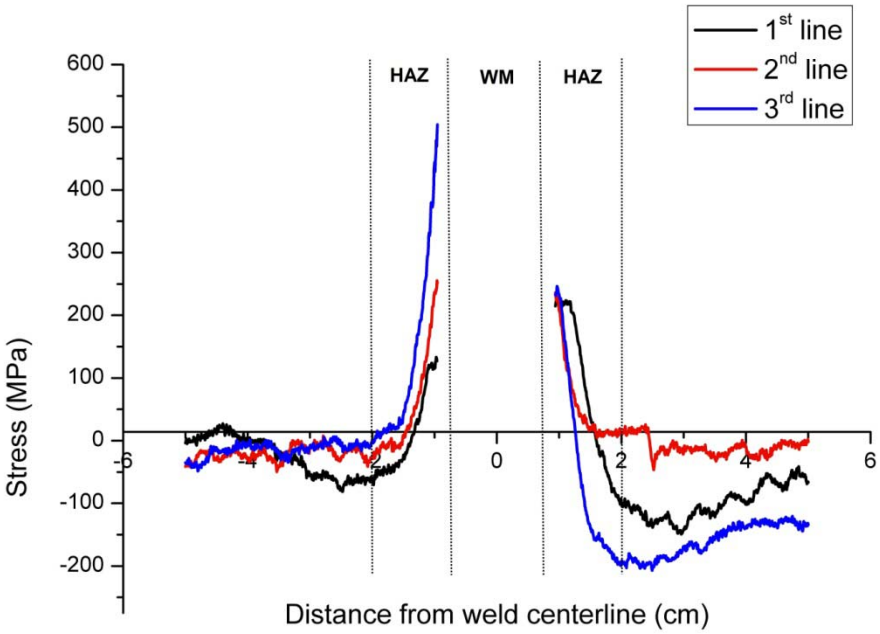

Figure 5.17: Longitudinal residual stress distribution of API 5L X70 (12 mm) steel from surface at measurement lines 1-3.

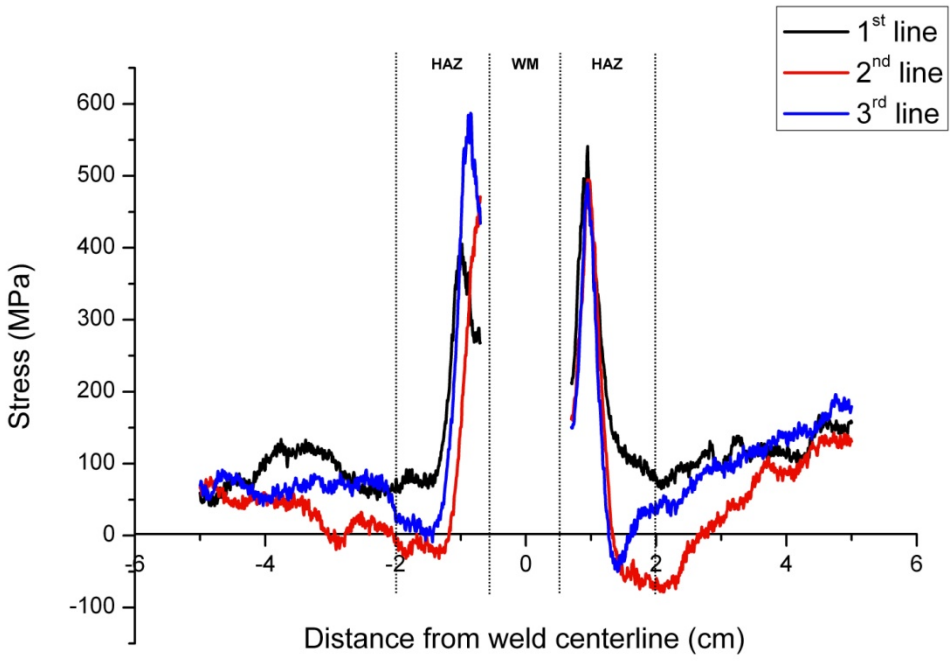

a)

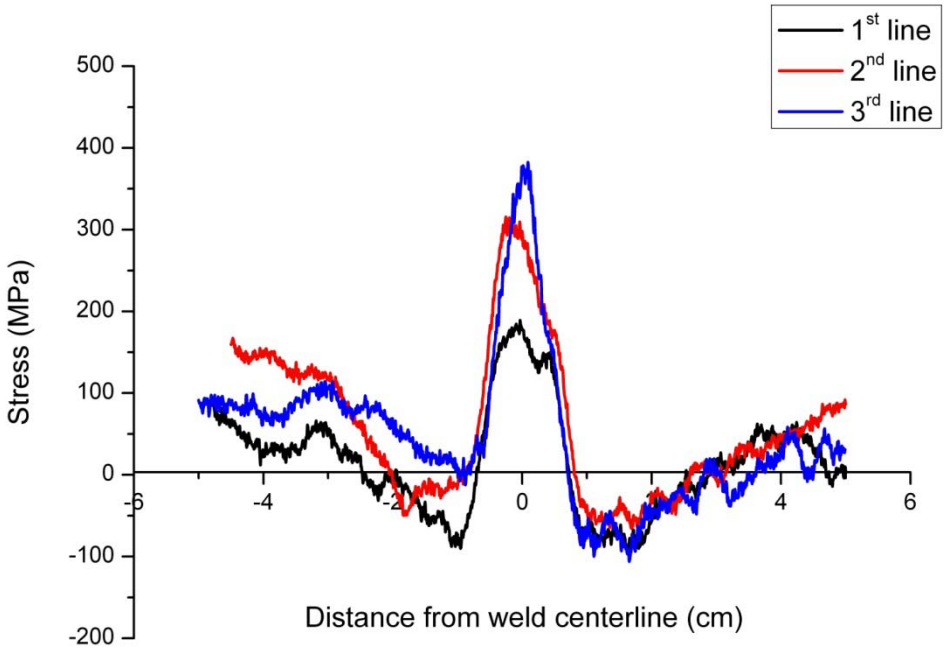

b)

Figure 5.18: Longitudinal residual stress distribution of API 5L X70 (15 mm) steel from a) surface and b) back surface at measurement lines 1-3.

Residual stress distribution of four different plates shows similar tendencies among each other and also with earlier studies in literature.

In their study Kesevan et al. also found a similar longitudinal residual stress distribution for 6 mm. thickness mild steel sample as shown in Figure 5.19 from front surface of the plate. Initially plate has compressive residual stress region and after welding these compressive stresses were changed to tensile stresses which reach maximum at weld centerline.

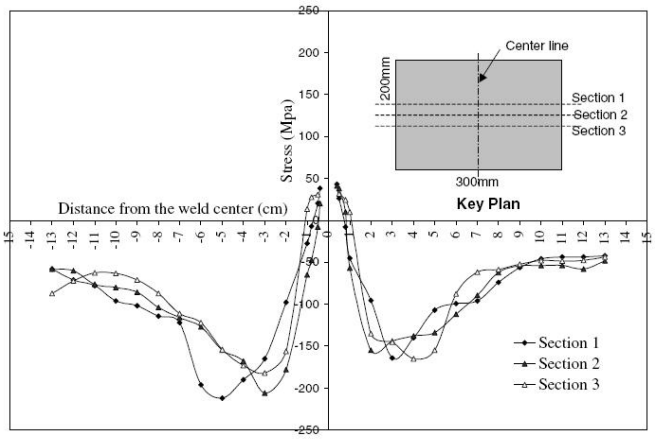

Figure 5.19: Longitudinal residual stress distribution for mild steel sample [28]

Ju et al. used two different calibration methods in their study. They found that HAZ based calibration method is more reliable than base metal based calibration method.

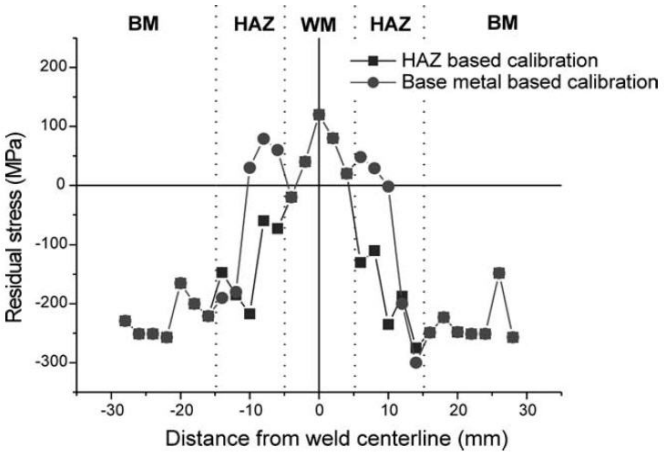

Figure 5.20: Longitudinal residual stress distribution for API X65 plate [29]

5.5. MBN Results for HAZ Based Calibration

The second calibration technique was the HAZ based calibration technique. Figure 5.21 represents the residual stress results of 15 mm P355NL2 steel from its front surface. It is observed that a shift in residual stress results occurred at HAZ regions by using HAZ based calibration technique. This shift is caused by the microstructural changes in the plate that occurred as a result of welding. Since MBN values are also sensitive to microstructural changes the literature shows that HAZ based calibration method is more accurate than the base metal calibration technique [20]. In this study the calibration sample was prepared from HAZ region and represents only a microstructural region. However, for each different microstructural region different calibration samples should be prepared for obtaining accurate results.

The similar increase in residual stress results was obtained for 12 mm API 5L X70 plate (Figure 5.22).

By comparing two different calibration method results, it was observed that welding introduces tensile residual stresses to the plates. Stress corrosion cracking is expected to occur at the regions where compressive stresses changed to tensile stresses rapidly.

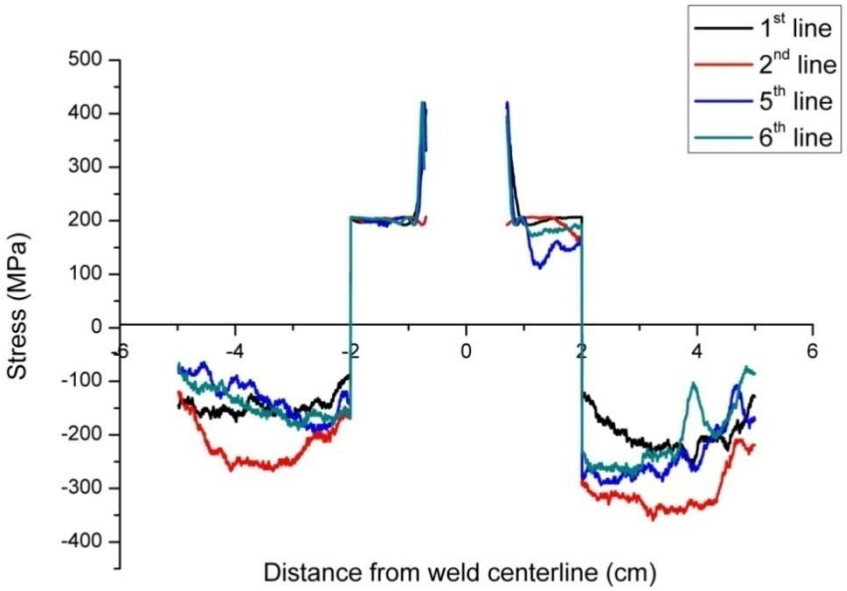

Figure 5.21: Longitudinal residual stress distribution of P355NL2 (15 mm) steel from surface at measurement lines 1, 2, 5 and 6 with HAZ based calibration.

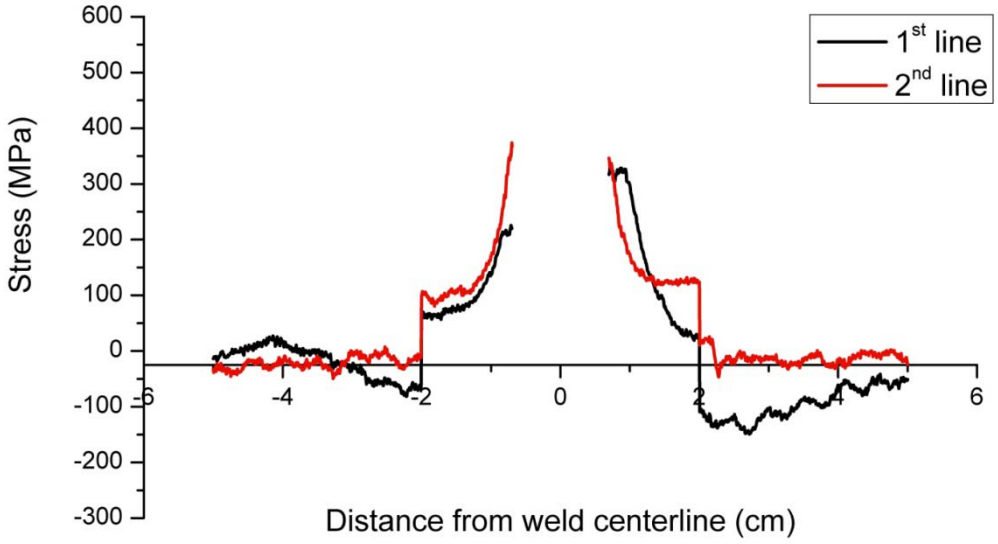

Figure 5.22: Longitudinal residual stress distribution of API 5L X70 (12 mm) steel from surface at measurement lines 2 and 3 with HAZ based calibration.

5.6. Verification of MBN results by Hole Drilling Method

Hole drilling method is one of the most used techniques for residual stress measurements and defined as semi-destructive method since the drilled hole diameter is very small. ASTM E837-01 standard defines the general overview of residual stress measurements by hole drilling method. Hole drilling measurements were conducted on 15 mm API 5L X70 plate from its back surface. Integral method was used for obtaining residual stress values. The first measurement point was the centerline of the weld and second measurement point was 32 mm away from the first point. At each drilling step which was 0.1 mm, relieved strains were measured with strain gauges and then changed to stress values by elastic laws. Measurement results gave a reasonable correlation with Magnetic Barkhausen noise technique. The high deviation occurred at in Figure 5.24b for maximum stress line was resulted from a broken drilling bit. So the results from 0.3 mm can be neglected.

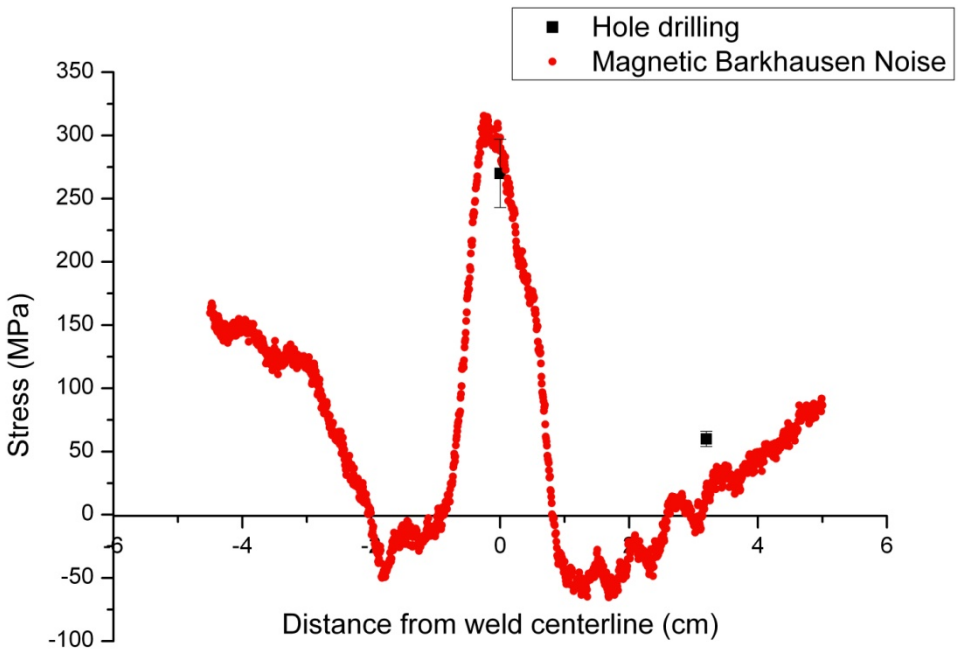

Figure 5.23: Comparison between hole drilling and Magnetic Barkhausen noise technique results for 15 mm API 5L X70 steel from the back surface (2nd line) of the plate

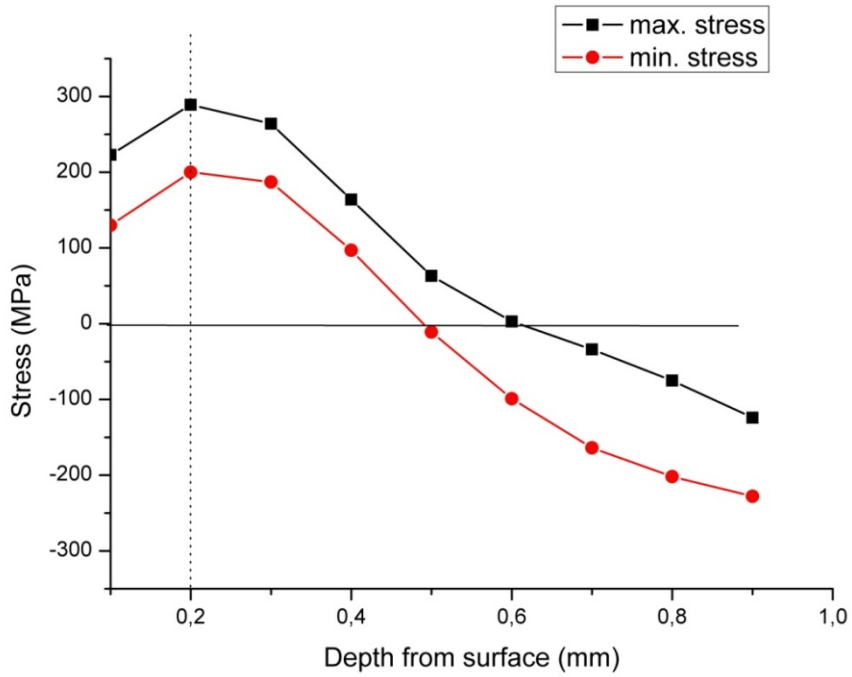

a)

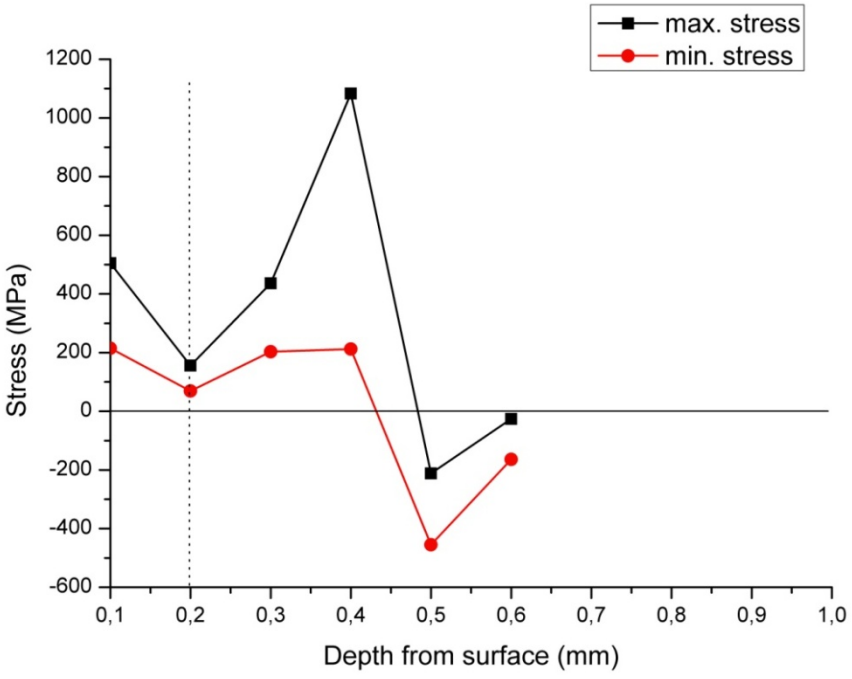

b)

Figure 5.24: Depth profile of residual stresses obtained from the back surface of 15 mm API 5L X70 plate by hole drilling method a) first gauge b) second gauge

CHAPTER 6

CONCLUSIONS

Magnetic Barkhasuen Noise (MBN) measurements on the heat affected zone and parent metal of the single pass welded plates were carried out. For this aim, a MBN-residual stress calibration set-up and a measurement system with scanning ability was developed. The results were verified by the hole-drilling measurements, microstructure investigation and hardness measurements.

The following conclusions can be drawn from the results.

- According to microstructure investigation four different microstructural regions were observed for each plate which affects the residual stress distribution.
- Welding introduces high tensile residual stress to the plates at heat affected zones (HAZ) and weld metal regions. These stresses are the main causes of stress corrosion cracks and fatigue cracks.
- The decline occurred at the HAZ regions of plates from front surface results are due to the effect of grain coarsening occurred at CGHAZ (coarse grained HAZ) region. The decline of tensile residual stress values occurred at the centerline of the weldment from back surface results are due to the combination effects of shrinkage, transformation and quenching.

- Calibration procedure is very important for accurate and reliable results. Each zone having remarkably different microstructure should be separately considered for calibration.

- MBN technique is a very promising nondestructive technique for automated measurement of residual stresses on welded plates in a fast and reliable manner.

For further studies, multi pass welding can be used for generating more complex residual stress distributions. By measuring residual stresses after each pass, the effect of each pass on residual stress distribution for multi pass welded plates can be measured.

Also by applying different welding and material parameters different residual stress distributions can be generated. So by using different test specimens prepared by using different parameters, the effects of welding and material parameters can be measured with MBN technique.

Using bi-axial calibration rather than uni-axial calibration, which was used in current study, is also suggested for further studies to obtain more accurate results.

REFERENCES

[1] Mattis D. C., “The Theory of Magnetism Made Simple”, World Scientific Publishing, Singapore, (2006).

[2] Vowles, H. P., "Early Evolution of Power Engineering", *Isis* (University of Chicago Press) **17** (2): p.412–420, (1932).

[3] Withers P. J., Bhadeshia H. K. D. H., “Residual stress – Part 1-Measurement Techniques”, Mater Sci. Technol., 17, p.355 – 365, (2001).

[4] Chikazumi S., “Physics of Magnetism”, Wiley, New York, (1964).

[5] Rahim T., “The Effect of Plastic Deformation and Residual Stress on Magnetic Barkhausen Noise And Magnetic Flux Leakage Signals For Mild Steels”, MSc. Thesis, (2003).

[6] Cullity B.D., “Introduction to Magnetic Materials”, Addison-Wesley, Reading, (1972).

[7] Neelkanta P.S., “Handbook of Electromagnetic Materials: Monolithic and Composite Versions and Their Applications”, CRC Press, Boca Raton, Florida, (1995).

[8] Durin G., Zapperi S., “The Science of Hysteresis", vol. II, G. Bertotti and I. Mayergoyz eds, Elsevier, Amsterdam, p.181-267, (2006).

[9] Jiles D., “Dynamics of Domain Magnetization and the Barkhausen Effect”, Czechoslovak Journal of Physics, 50, p.893-988, (2000).

[10] Jiles D., “Introduction to Magnetism and Magnetic Materials”, Chapman and Hall, London; New York, (1991).

[11] Willcox M., Mysak T., “An Introduction to Barkhausen Noise and its Applications”, Insight NDT Technical Booklet, (2004).

[12] European Network of Surface and Prestress Engineering and Design Website (http://www-ensped.utt.fr/aboutprestress/definition.htm).

[13] Macherauch E., Kloos K.H., “Origin, Measurements and Evaluation of Residual Stresses”, Residual Stresses in Science and Technology, DGM Inform., Verlag, p.3-26, (1987).

[14] American Society of Welding Website (www.aws.org).

[15] Nitscke-Pagel Th., Wohlfahrt H., “The Generation of Residual stresses due to Joining Processes, Residual Stress – Measurement, Calculation, Evaluation”, DGM Informationsgesellschaft, p.121-134, (1991).

[16] Masubuchi K., “Residual Stress and Distortion”, Metals Handbook, Vol 6, Welding, Brazing and Soldering, ASM, (1983).

[17] ASM Metals Handbook Volume 6, Welding, Brazing and Soldering, ASM, (1993).

[18] Degarmo E.P., Meriam J.L., Jonassen F., “The Effect of Weld Length upon the Residual Stress of Unstrained Butt Welds”, Welding journal, 25, p.485-486 (1946).

[19] Gür C.H.,”MetE 462 Residual Stress lecture notes”, METU, (2008).

[20] Lu J., “Handbook of Measurement of Residual Stresses”, Society for Experimental Mechanics, (1996).

[21] Grant P.V., Lord J.D., Whitehead P.S., “The Measurement of Residual Stresses by Incremental Hole Drilling Technique” Measurement Good Practice No:53, National Physical Laboratory, United Kingdom, (2002).

[22] Prevéy P. S., “X-ray Diffraction Residual Stress Techniques,” Metals Handbook, 10, Metals Park American Society for Metals, p.380-392, (1986).

[23] Kudryavtsev Y., Kleiman J., Gushcha O., “Residual Stress Measurement in Welded Elements by Ultrasonic Method”, IX International Congress on Experimental Mechanics, Florida, USA, p.954-957, (2000).

[24] Leggatt R.H., “Residual Stress in Welded Structures”, International Journal of Pressure Vessels and Piping, 85, p.144–151, (2008).

[25] Withers P. J., Bhadeshia H. K. D. H., “Residual Stress – Part 2- Nature and Origin”, Mater Sci. Technol., 17, p.366 – 375, (2001).

[26] Masubuchi K., “Research Activities to Examine Residual Stresses and Distortion in Welded Structures”, Welding Journal, 70, p.41-47, (1991).

[27] Gauthier J., Krause T. W., Atherton D. L., “Measurement of Residual Stress in Steel Using the Magnetic Barkhausen Noise Technique”, NDT&E International, Vol. 31, No. 1, p.23-31, (1998).

[28] Kesavan K., Ravisankar K., Parivallal S., Sreeshylam P., “Non Destructive Evaluation of Residual Stresses in Welded Plates Using the Barkhausen Noise Technique”, Experimental Techniques, p.17-21, (September/October 2005).

[29] Ju J.B., Lee S.K., Jang J., Kim W.S., Kwon D., “Determination of Welding Residual Stress Distribution in API X65 Pipeline Using a Modified Magnetic Barkhausen Noise Method”, International Journal of Pressure Vessels And Piping, p.641-646, (2003).

[30] Stewart D.M., Stevens K.J., Kaiser A.B., **“**Magnetic Barkhausen Noise Analysis of Stress in Steel”, Current Applied Physics, 4, p.308-311, (2004).

[31] Lindgren M, Lepisto¨ T. “Residual Stress Evaluation in Welded Steel Tubes Using Barkhausen Noise”. Conference Proceedings of Barkhausen Noise and Micromagnetic Testing II,United Kingdom; 25–26: 91–100, (1999).

[32] Ochodek V., “Residual Stress Evaluation in Spirally Welded Pipes for Gas Pipelines”, 6th International Conference on Barkhausen Noise and Micromagnetic Testing, (2007).

[33] Ochodek V., “Measurements of Residual Stress by Magnetoelastic Method on X70 Gas Pipes”, Research report of VSB Technical University Ostrava, (2006).

[34] McIntire P., Birks A. S., Green, Jr. R. E., “Nondestructive Testing Handbook”, Volume 7, Ultrasonic Testing, ASNT, p.830, (1991).